Chapter - 5

Gain Enhancement of Hexagonal UWB Antenna using AMC

5.1. Introduction

As mentioned in chapter 1 of the thesis, the main advantage of patch antenna is its low profile. Another advantage is the ease of fabrication when fed with probe at desired location as discussed in chapter 2 of the thesis. This chapter utilized the ground reduction technique as demonstrate in chapter 3 of the thesis to achieve UWB. The AMC technique introduced in chapter 4 is exploited in this chapter for the gain enhancement of probe fed hexagonal monopole antenna.

Hexagonal monopole antenna generally exhibits low and non-uniform gain at lower S-band frequencies (Fallahi 2013) (Yadav 2017) (Shaalan 2010). This chapter presents a ground plane modification technique to achieve consistent and uniform gain for an S-Band monopole antenna. An S-band antenna covers applications as reflected in Table 5.1.

Table 5.1. Wireless communication systems frequencies covered by the S-band antennas

System	*Operating frequency (GHz)*
4G LTE (TD-LTE)	2.3–2.4 GHz (band-40)
LTE (FDD-LTE)	1.9–3.8 GHz (band-33 to band-43)
WiMAX	2.3–2.4 GHz (lower band) and 2.496–2.690 GHz (upper band)
Lower band of WiFi	2.412–2.4835 GHz
Bluetooth	2.402–2.480 GHz
Lower 5G bands	3.3–4.2 GHz and 4.4 – 4.9 GHz

Demand of economic AMC are increasing for filtering radio waves from wireless communication systems such as WiMAX, WLAN, and X-Band (Bashiri 2017). AMC are also utilized for bandwidth and gain enhancement of the low profile antenna (Addaci 2016). Peak Gain of the UWB monopole antenna may be enhanced through AMC techniques such

as given in (Tahir 2017) (Tahir 2016) (Ram Krishna 2015) (Ram Krishna 2014) (Dewan 2017). The AMC reflector technique can also be utilized as demonstrated in (Dewan 2017) (Hosseinipanah 2010), to improve the peak and the boresight gain of the antenna. AMC applications are growing rapidly and its analysis techniques are less explored. It is necessary to analyze the square loop AMC with different inner widths in order to analyze its effect on the transmittance characteristics for two different modes of incidence.

Hexagon and its derivatives are utilized to cater the wideband demand (Li 2014), but higher modes with low boresight gain are excited (Joshi 2018). Various techniques are available in literature to enhance the peak gain of patch antenna (Tahir 2017) (Ranga 2013) (Krishna 2015) (Park 2013), which increase the volume or area of the antenna, but the boresight gain enhancement is rare in the literature (Zhang 2012). Simpler or a straightforward technique to increase antenna gain at boresight is not much explored in literature. A technique is essential to be identified to overcome the issue of low boresight gain in low profile S-band patch antenna.

Modified ground structures are used to enhance the bandwidth and gain of the printed antenna (Jhajharia 2018). The ground modification can be a potential simpler solution to enhance the boresight gain of the antenna by exciting lower order mode as well as provide wide radiation bandwidth. Modified ground technique is chosen in this chapter over other techniques for practical simplicity, to enhance the impedance bandwidth and gain of the antenna to avoid any further increase in size as well as the volume of the antenna and to maintain ease of fabrication and connection as the case for probe fed antenna.

In this chapter, a novel modified ground design for printed S-band antenna is reported. The designed antenna is composed of hexagonal patch backed with a semi elliptical ground that is excited through a probe. The rectangular slot is etched near the probe into the semi elliptical ground. The chapter compares an antenna performance with and without connector

flanges. The removal of connector flanges is treated here as a part of ground plane modification technique. This chapter explains how the modified ground improves matching of impedance for a flangeless connector fed antenna. The effect of absence and presence of connector flanges is explained through measurements in this chapter. The effect of modified ground and connector flanges on boresight gain, peak gain and the radiation pattern is elaborated and discussed in this chapter.

Printed antennas for UWB application are used for compact and portable devices due to low profile and easy integration. Printed monopole antennas with microstripline feed such as circle, ellipse, square, pentagon and hexagon are used for UWB application (Liang 2005) (Liu 2011) (Ram Krishna 2015) (Mao 2014) (Ray 2010) (Kumar 2002). Different higher order modes can be easily excited using hexagonal geometry as the patch when fed at vertex of hexagon (Joshi 2016c) (Joshi 2015d). Antenna with monopole characteristics such as impedance and radiation can be achieved by reducing ground plane (John 2008). In order to transform a dipole antenna to a monopole antenna the ground plane can be reduced as reported in (Joshi 2017). The introduction of the slots on the ground plane or on the radiator can minimize the ground plane effect on UWB monopole antenna (Lu 2011) (Ellis 2015) (Chen 2007). Ground plane reduction can improve impedance matching for a desired mode while suppressing some other undesired or spurious radiation. It is necessary to analyze the effect of ground plane reduction in order to address issues posed by coaxial probe feeding before designing a direct-fed monopole hexagonal patch antenna for UWB applications.

To design a hexagonal printed UWB antenna, the mode theory applied to a circular radiator using the cavity model, the ground reduction technique and the monopole configuration are utilized in this chapter. A vertex-fed hexagonal UWB antenna is designed, fabricated and characterized using experiments and measurements. Different modes are excited by choosing an appropriate feed location that can excite diverse modes uniformly.

The gain of the antenna is controlled by the introduction of a concentric hexagonal slot in the patch. The ground plane reduction technique is utilized to transform the dipole antenna to the monopole like antenna. The monopole antenna with slotted ground is used to improve the impedance bandwidth of the antenna. The main objective of this chapter is to demonstrate the ultra wideband hexagonal antenna by using a rigid coaxial waveguide or probe. The SMA connector used in this work is modified by the removing its flanges. The experimental results verify that the technique suits to design and develop an UWB antenna.

A simple technique is presented to design a probe fed hexagonal monopole antenna when feed is along the vertex of hexagon. In this technique, the lowest edge resonant frequency formula for stripline fed hexagonal monopole antenna is modified and used to calculate the lowest edge resonant frequency of probe fed hexagonal monopole antenna. The empirical formula available in literature are modified to achieve better accuracy and low error for the calculation of lower edge frequency of stripline fed monopole antennas. Empirical formula for the calculation of the lower edge frequency for probe fed planar monopole antenna is derived and presented. The presented empirical formula is further validate using simulation and measurement results for the probe fed hexagonal monopole antenna.

Most of the UWB antennas have a monopole configuration, so it is necessary to analyze the effect of geometry of the ground plane on the reflection and radiation characteristics of the hexagonal antenna when directly fed by a coaxial connector to achieve UWB. A direct-fed hexagonal ultra wideband antenna using flangeless SMA connector is proposed. Further, an antenna prototype is developed and characterized through measurements. The effect of absence of connector flange on the reflection characteristics, the radiation characteristics and the farfield gain is also presented.

The AMC reflector technique is utilized in this chapter as demonstrated in (Dewan 2017) (Hosseinipanah 2010), to increase antenna's peak gain as well as gain at its boresight of the

hexagonal monopole antenna. An AMC reflector is chosen over parasitic ground (Zhang 2012) to maintain stability in shape of radiation pattern at higher frequencies as well as convenience of assembling it with a pre-developed antenna.

A probe fed UWB patch antenna with AMC reflector is demonstrated. The effect of reflector on antenna farfield gain of the designed antenna is analyzed and studied. The antenna and AMC, both are developed on thin FR-4 dielectric substrate while polystyrene is used as spacer between the antenna and AMC. A method to improve the farfield gain, by keeping loop AMC reflector and probe fed UWB antenna together is presented. The motivation towards this work is to demonstrate a technique to procure an enhancement in average peak gain > 3 dB at higher UWB frequencies of a fabricated hexagonal monopole antenna. An AMC reflector array with a square loop unit cell becomes suitable choice to boost the peak gain of any pre-fabricated UWB monopole antenna.

It is significant to note that the quarter wave probe fed hexagonal antenna when fed at the vertex is used throughout the chapter. Section 5.2 presents uniform gain realization in probe fed hexagonal monopole antenna. In section 5.3, probe fed hexagonal UWB antenna is demonstrated. Empirical formula to calculate the lower edge frequency of the hexagonal monopole antenna is also presented.

5.2. S-Band Monopole Antenna with Modified Ground Plane

The antenna structure with flangeless connector and its design schematic are described in this section. The initial schematic design involves an antenna having a slotted hexagonal patch and a square ground plane with dimension 40 × 40 mm^2 ($L_g \times L_g$) as shown in Figure 5.1(b) and 5.1(c). The optimized hexagon dimensions are 33 mm × 28.57 mm which is suitable for monopole antenna design. Further, the ground plane is modified by reducing the length of ground plane by 92.5% and adding a half ellipse with a minor radius of e_r = 2.5 mm to it, as

reflected in Figure 5.1(d) and 5.1(e) respectively. The overlapping of the patch and the ground plane is avoided by shifting the whole ground towards left by 2 mm as may be observed from Figure 5.1(d) and 5.1(e), thus antenna exhibits monopole characteristics. A rectangular slot of 2×10 mm^2 dimension is also etched in reduced rectangular ground plane, modified ground plane geometry is shown in Figure 5.1(f). The antenna is constructed over a FR-4 substrate with dielectric constant = 4.3, height (h) = 1.5 mm, L_s = 46 mm, and tan δ = 0.025 as depicted in Figure 5.1(a). The antenna is fed through a probe near the vertex of the hexagonal patch as shown in Figure 5.1(a) and 5.1(b).

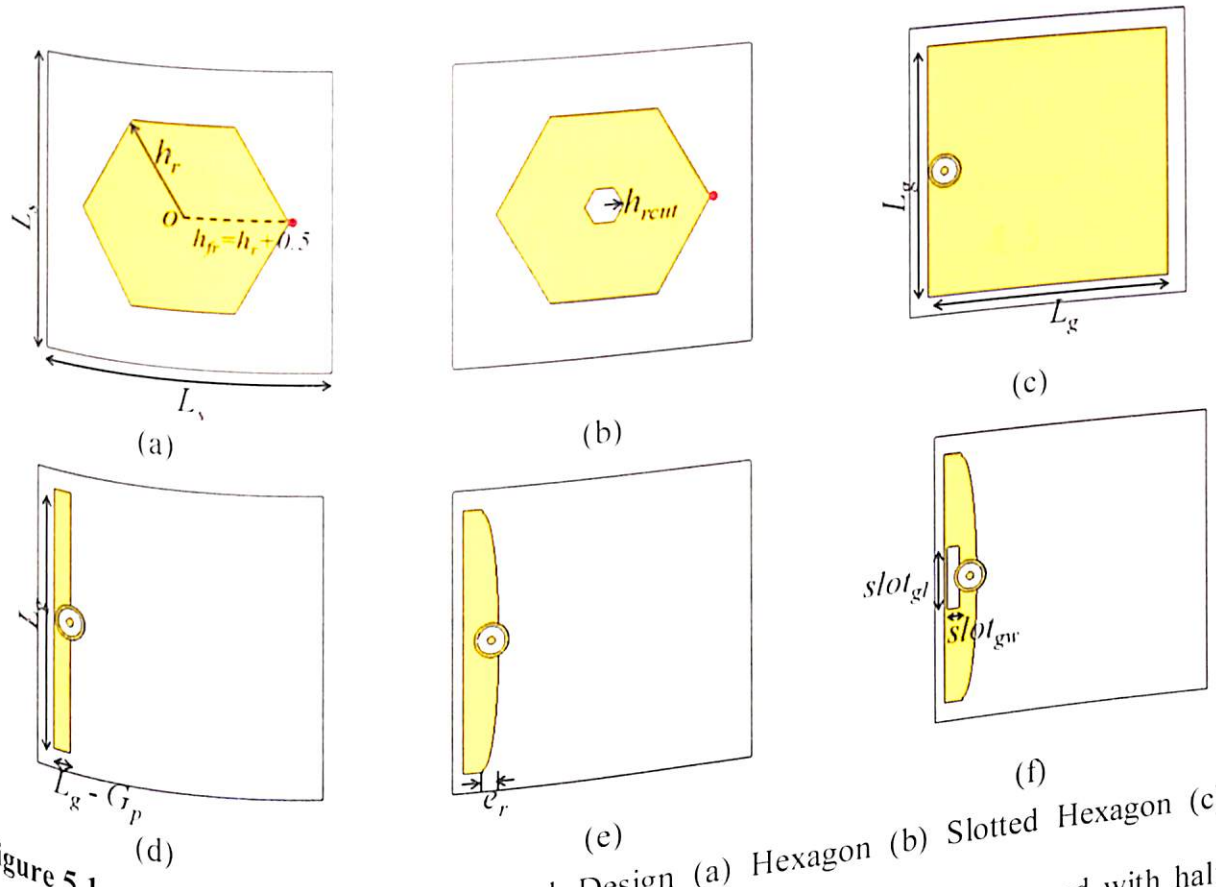

Figure 5.1. Evolution of the Proposed Design (a) Hexagon (b) Slotted Hexagon (c) Ground used for (a) and (b) (d) Reduced Ground with (b) (e) Reduced ground with half ellipse (f) Proposed modified ground.

The evolution of the proposed design is shown in Figure 5.1 and change in reflection coefficient, $|S_{11}|$ (dB) during it, is shown in Figure 5.2. The modified geometry of the ground plane supports impedance matching to excite lower frequency in antenna radiation. The

modified ground drags the two frequencies closer and consequently forms a wide band from 2.3 GHz to 4.6 GHz as observed from Figure 5.2. When the ground is modified, the reactive components, i.e. mainly patch capacitance changes, which help in matching the characteristics impedance of the antenna.

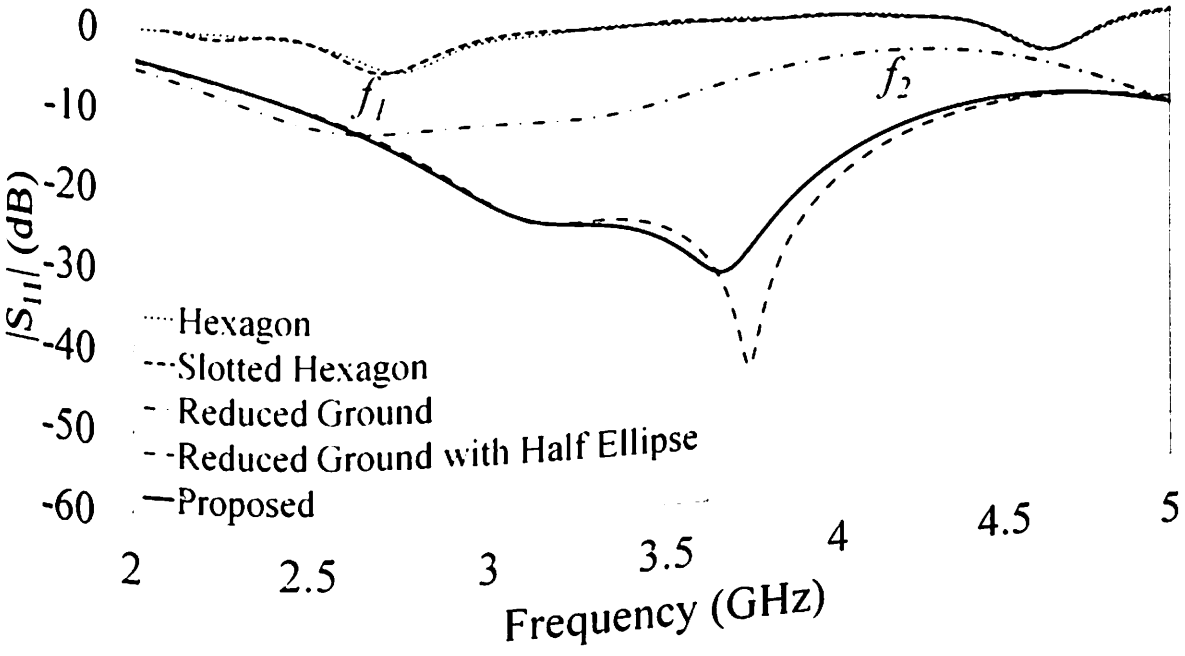

Figure 5.2. $|S_{11}|$ (dB) analysis of Evolution of the proposed design.

The evolution of the designed antenna gain analysis suggests that when a dipole antenna is transformed into a monopole design, the ripples in the gain performance are reduced tremendously and uniformly distributed positive gain is achieved, as evident from Figure 5.3. Dipole peak gain characteristics is shown by full hexagon with square ground at 2.3 GHz. Gain ripples at 3 GHz and 4 GHz in slotted hexagon are obtained due to the radiation of the slot. The reduction of ground plane raises the gain at higher frequencies which helps in attaining positive gain. The reduced ground with half ellipse reduced the ripple between 2.5 GHz and 4 GHz. The introduction of the rectangular slot in reduced ground with half ellipse leads to the proposed modified ground and provide the uniform gain characteristics as may be observed in Figure 5.3. The peak gain increases after 4.6 GHz, due to increase in effective

area with frequency of the designed antenna. The boresight gain reflects negative value after 4.6 GHz because of the presence of various modes of antenna configuration which consequently leads to certain destructive interference and reflects in form of multiple squinted beams in gain pattern at higher frequency. The uniform and flat gain of the proposed antenna design within operating S-Band makes the antenna suitable for S-Band applications.

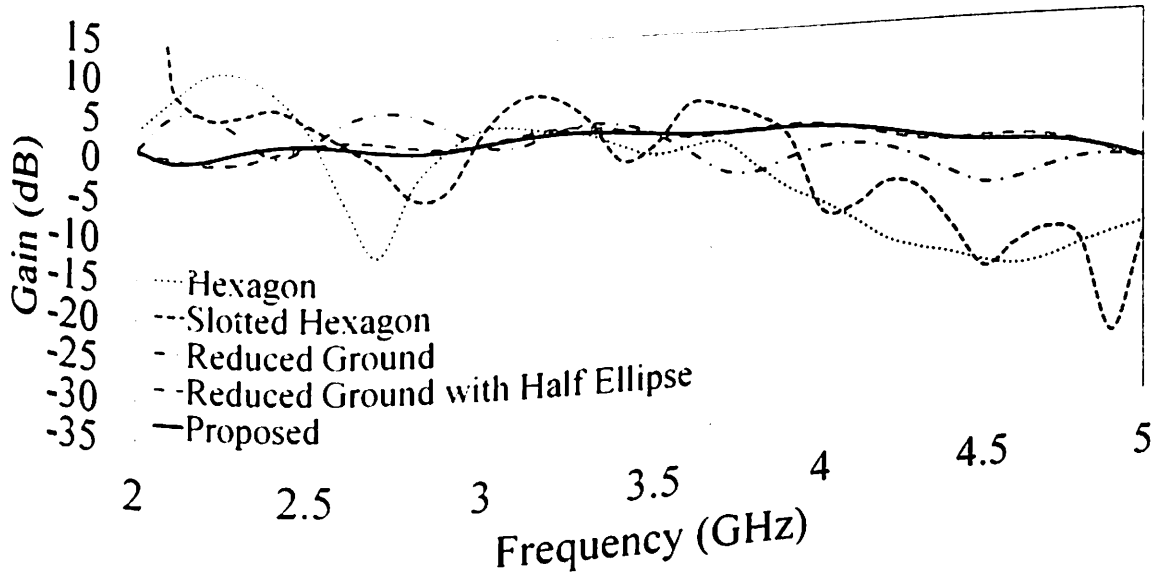

(a)

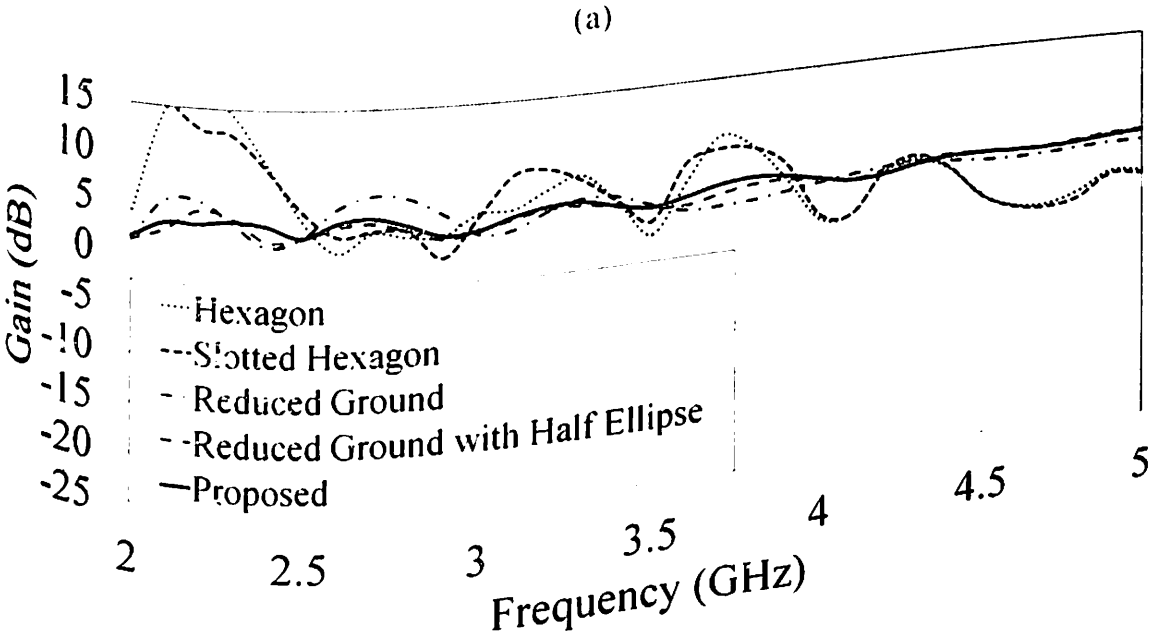

(b)

Figure 5.3. Gain analysis of Evolution of the proposed design (a) Boresight Gain (b) Peak Gain.

In order to analyze the sensitivity of the designed antenna in its performance due to fabrication inaccuracies, the antenna design parameters such as antenna feed point (h_{fr}), ellipse radius (e_r) and ground slot dimension ($slot_{gl}$ and $slot_{gw}$) are observed by varying its value. Initially, h_{fr} is observed by varying it from 15 mm to 17 mm with a step of 0.5 mm in order to check $|S_{11}|$<-10 dB sensitivity within S-band and the presence of both the frequencies as reflected in Figure 5.4. The antenna $|S_{11}|$ is quite sensitive towards the feed point location to operate within the S-band. Change in feed point switches between the dominance of f_1 and f_2 frequencies, but lower band extremes are observed to be almost stable. 17 mm is chosen to avoid $|S_{11}|$>-10 dB at higher frequency within the operating band, after antenna prototype fabrication.

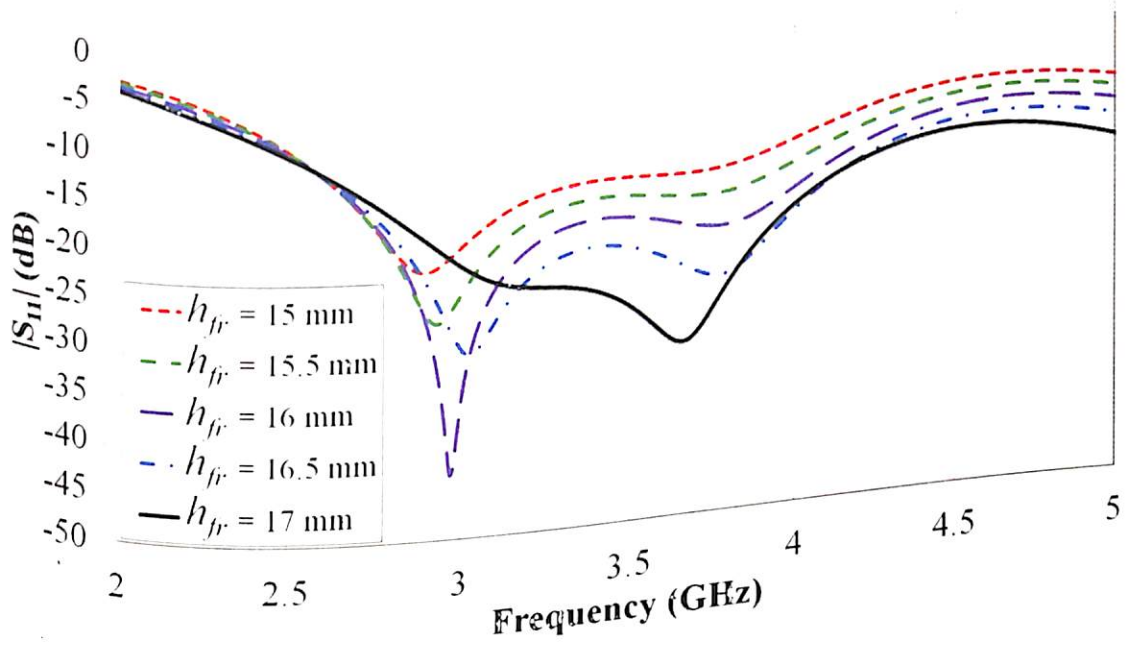

Figure 5.4. Reflection coefficients (S_{11}) for different values of h_{fr}.

The antenna performance sensitivity due to the minor radius of the half ellipse on $|S_{11}|$ and the gain is analyzed. The minor radius of the half ellipse e_r is varied from 1.5 mm to 3.5 mm with a step of 0.5 mm and variation in $|S_{11}|$ and antenna gain due to radial change are presented in Figure 5.5 and Figure 5.6 respectively.

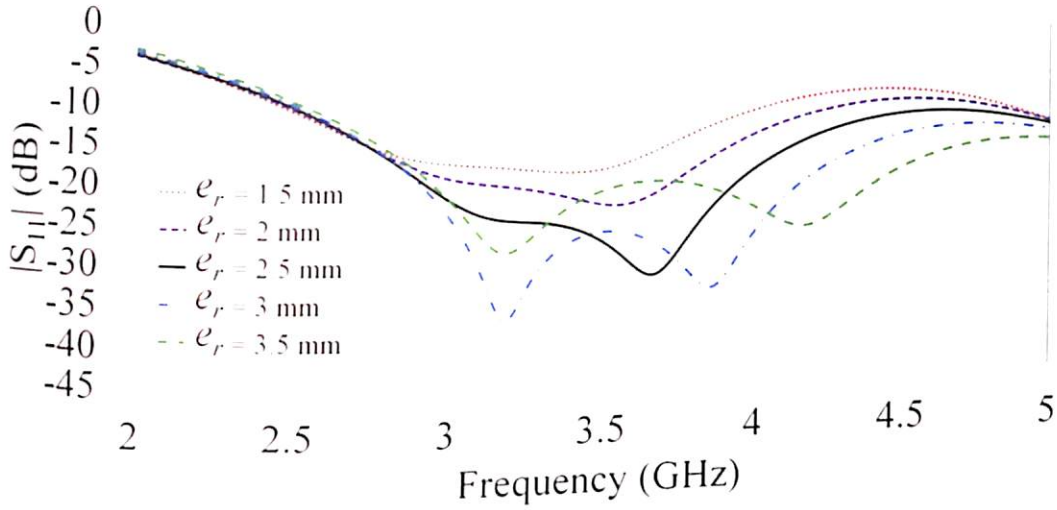

Figure 5.5. $|S_{11}|$ (dB) performance of S-Band antenna versus e_r

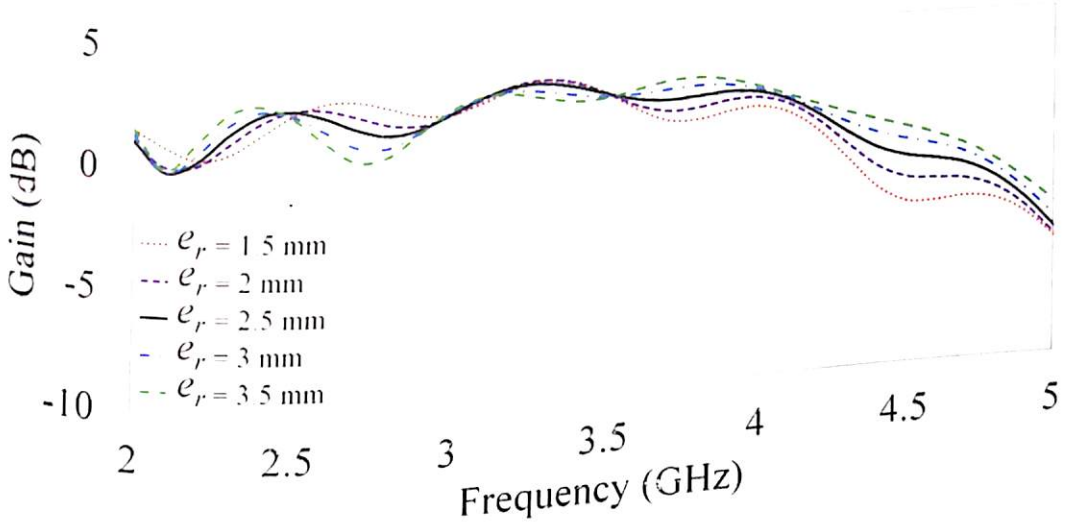

(a) Boresight Gain

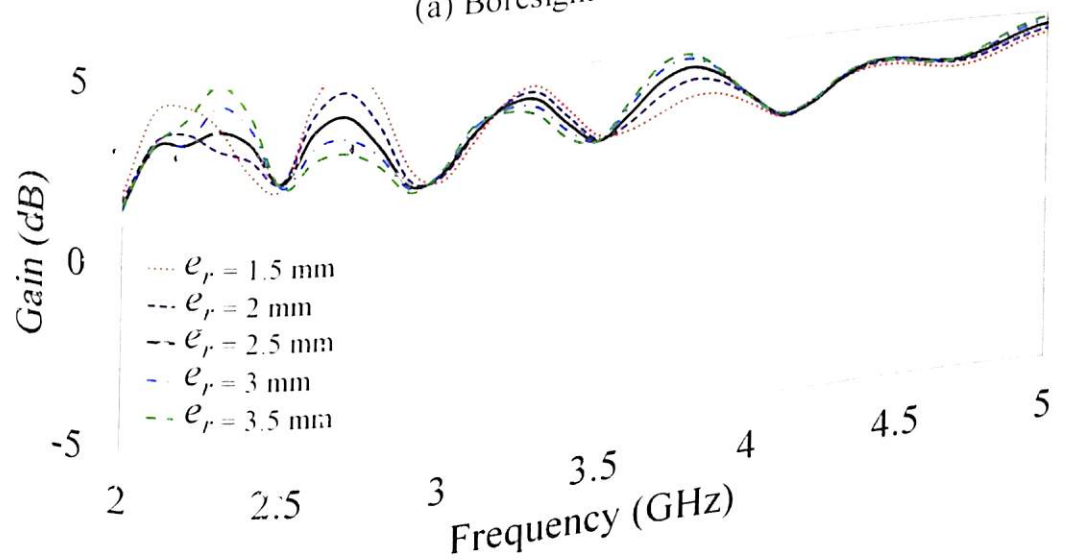

(b) Peak Gain

Figure 5.6. Gain performance of S-Band antenna versus e_r.

An increase in the circumradius of semiellipse do not bring much difference in ripples in antenna boresight as well as peak gain between 2 GHz and 4 GHz, but suitable value e_r = 2.5 mm is chosen as a trade off ensuring a monopole radiator design.

The dimensions of the rectangular slot in the ground is quite sensitive to gain performance as shown in Figure 5.7 and Figure 5.8. The width of the slot, $slot_{gw}$ and the slot length, $slot_{gl}$ as shown in Figure 5.1(f) are varied between $8 \leq slot_{gw} \leq 12$ mm and $1 \leq slot_{gl} \leq 3$ mm respectively. Not much change is observed in $|S_{11}|$ versus frequency plot shown in Figure 5.7. The effect of slot dimensions ($slot_{gl} \times slot_{gw}$) on the gain characteristics of the designed antenna with h_r = 17 mm, h_{rcut} = 3 mm and G_p = 37 mm is shown in Figure 5.8. Introduction of slot ensures a uniformity in antenna gain throughout its operating band. The peak and the boresight gain are uniform and positive when $slot_{gw}$ and $slot_{gl}$ are 10 mm and 2 mm respectively and further variation may lead to ripples in gain characteristics of the antenna.

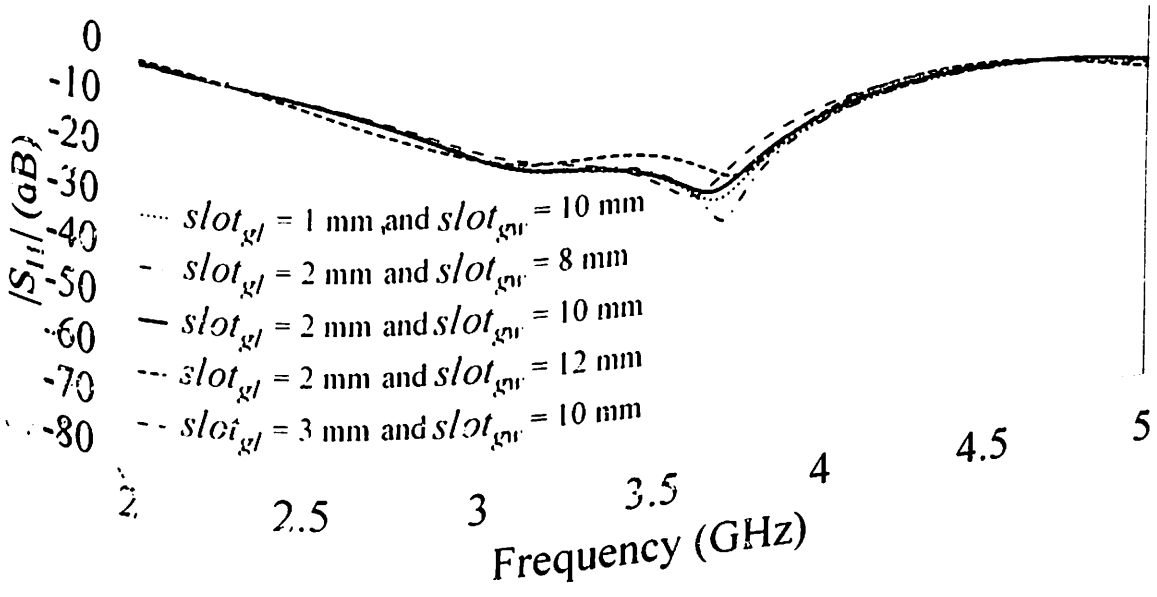

Figure 5.7. $|S_{11}|$ (dB) performance of S-band antenna versus $slot_{gl}$ and $slot_{gw}$.

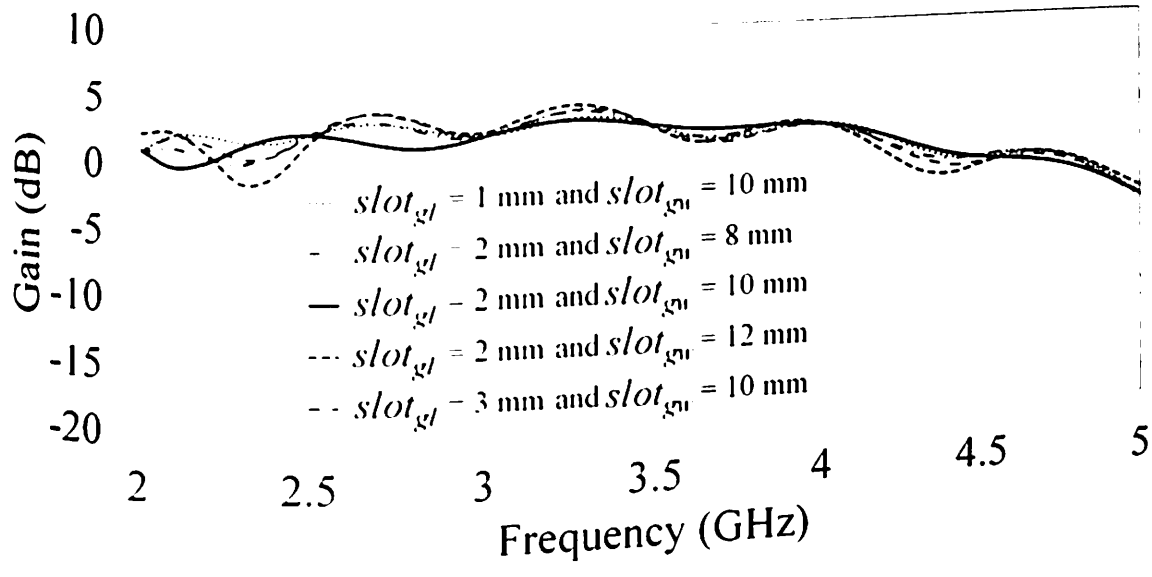

(a)

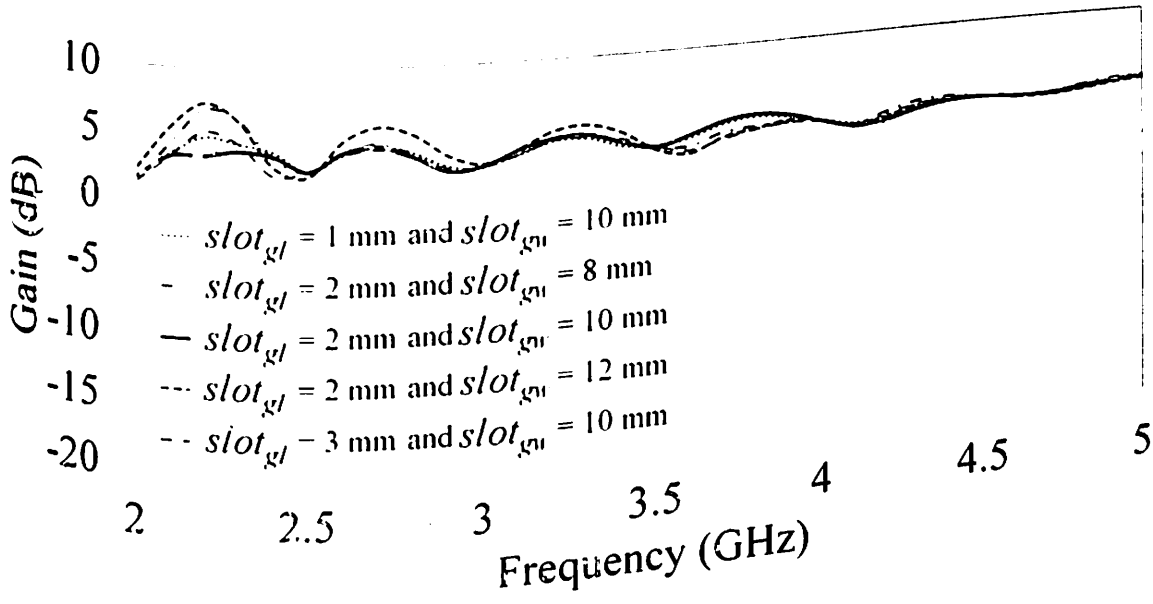

(b)

Figure 5.8. Gain performance of S-Band antenna versus $slot_{gl}$ *and* $slot_{gw}$ (a) Boresight Gain (b) Peak Gain.

5.3. Hexagonal UWB Antenna

The design simulation results are also compared with experimentally measured results for proposed antenna design with and without flange in Figure 5.9. The antenna when fed through a connector with a flange exhibits C-band characteristics while when fed through a connector without a flange exhibits suitability towards UWB operation.

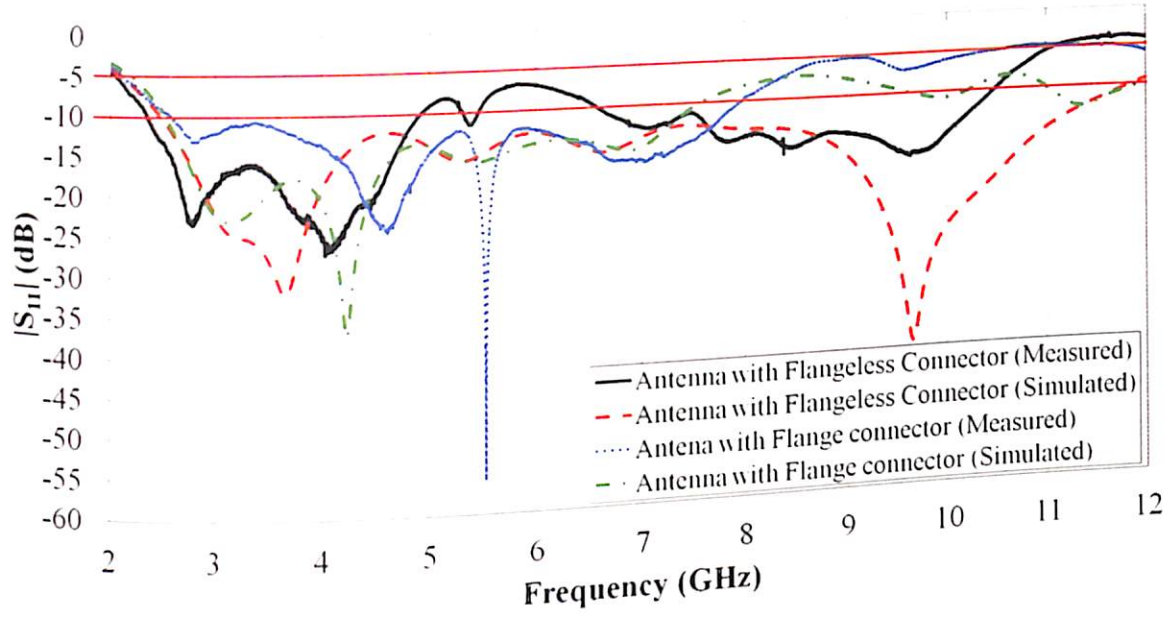

Figure 5.9. Scattering Parameter, $|S_{11}|$ (in dB) for probe fed hexagonal monopole UWB antenna.

A qualitative difference between the measurements and simulated results is observed due to the mechanical removal of the flanges from a standard SMA connector and tolerances during prototype fabrication. The measurements with antenna prototype show an impedance bandwidth ranging from 2.3 GHz to 10.6 GHz but with a band rejection of 1.6 GHz starting from 4.9 GHz to 6.5 GHz. Two notches are observed within the rejection range i.e. from 4.9 GHz to 5.3 GHz and 5.4 GHz to 6.5 GHz.

In order to achieve UWB characteristics, Bode-Fano criterion is utilized which states that to further increase the bandwidth for a given mode, the return loss is sacrificed (Pozar 2014). The diverse modes are accumulated and the return loss is decreased to enhance the bandwidth. In the design process of UWB antenna, various ground structures such as rectangular ground, trapezoidal ground and elliptical ground are simulated to observe wideband characteristics of the monopole antenna. Effect of rectangular and reduced ground plane do not exhibit UWB pattern as can be observed from discussions in earlier sections of the chapter. The effect of the trapezoidal and the elliptical ground with their best reflection

coefficients are compared and shown in Figure 5.10. The half-elliptical ground is chosen over trapezoidal ground in order to design the antenna, since better impedance matching is achieved over the entire UWB band.

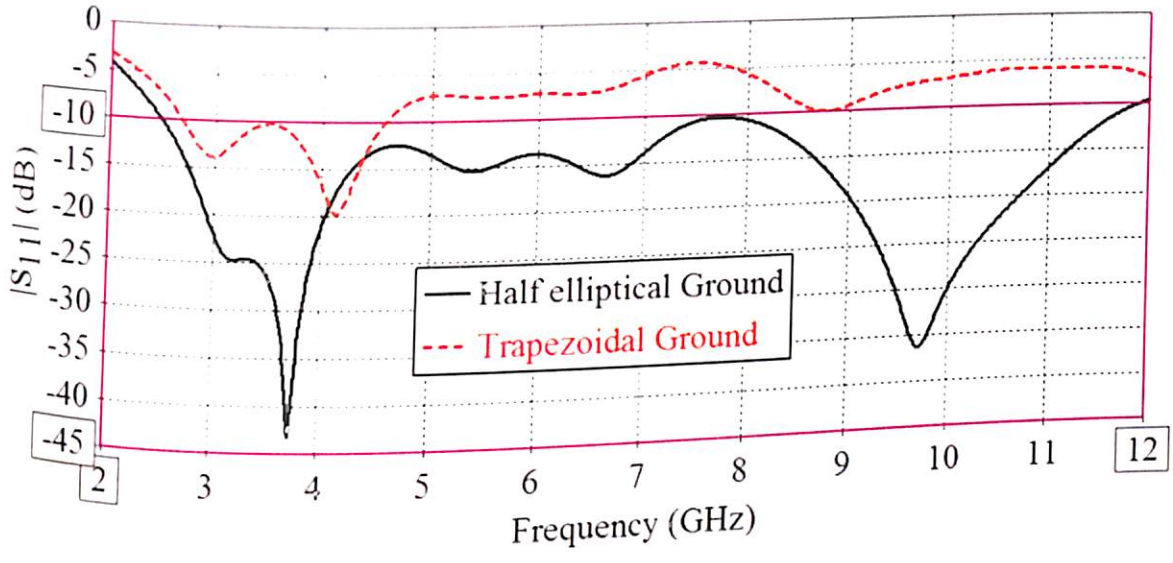

Figure 5.10. Reflection coefficients (S_{11}) for different ground structure when feed point is at 17.5 mm and r_{cut} is 3 mm.

A slot in half elliptical ground is introduced in order to further improve the reflection coefficient and remove the rejection band at 7.8 GHz. To optimize the dimension of the slot, the position of the slot is optimized through simulation, at 20 mm from the origin. The variation of the slot dimensions are shown in Figure 5.11. Figure 5.11 shows the optimized slot dimensions are 2 mm × 10 mm as the return loss increases around 7.8 GHz. Also, the circumradius of the hexagon is decreased from 17.5 mm to 16.5 mm and f_r is changed to 17 mm. The simulated results shows that the optimized design cover the complete UWB band from 2.4 GHz to 11.8 GHz.

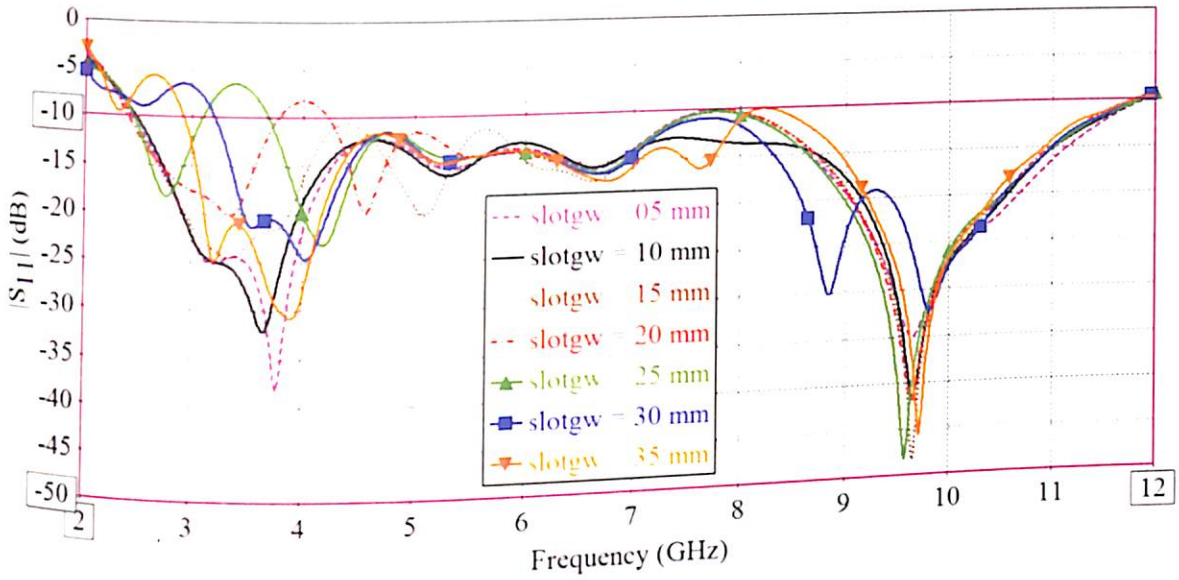

Figure 5.11. Reflection coefficients (S_{11}) for different values of slotwidth (slotgw) when slot length (slotgl) is 2 mm, feed point (f_r) is at 17 mm and r_{cut} is 3 mm.

Finally, the antenna design for UWB application is shown in Figure 5.12. To validate the results of the optimized design, the simulated results are compared with measurement results of the fabricated antenna as shown in Figure 5.13.

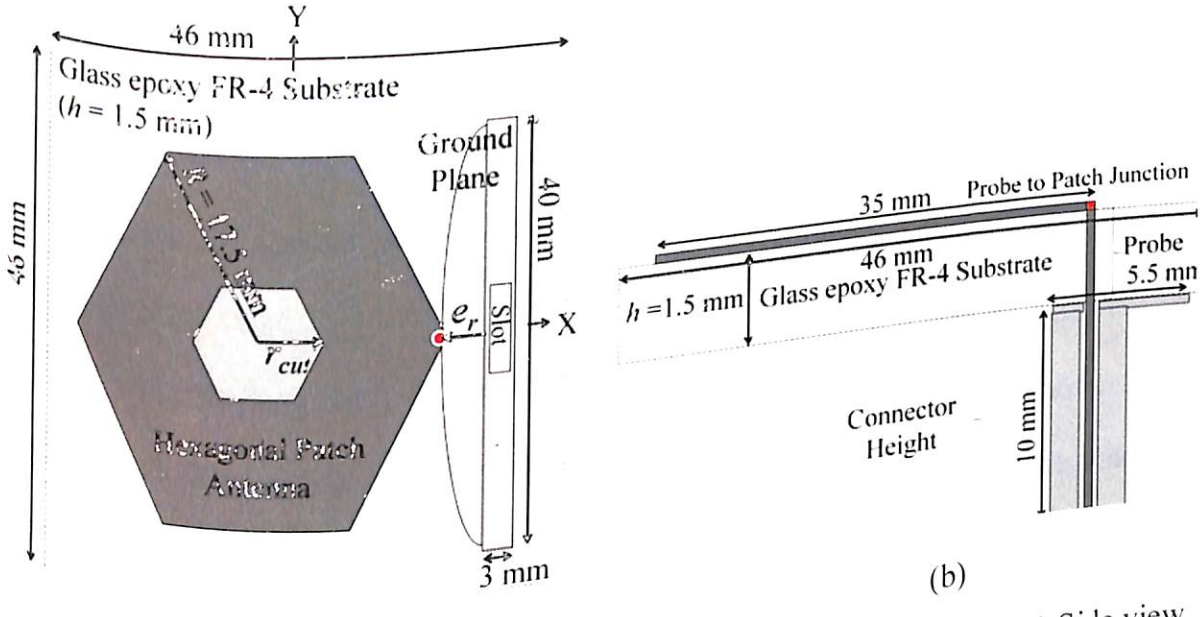

Figure 5.12. Proposed UWB Hexagonal antenna (a) Layout with dimension (b) Side view

There is a slight variation between the measurement reflection coefficient (dB) results due to the fabrication tolerances and manual modification of the probe. The measured results show the impedance bandwidth from 2.4 GHz to 10 GHz which covers almost whole of the band required for UWB applications.

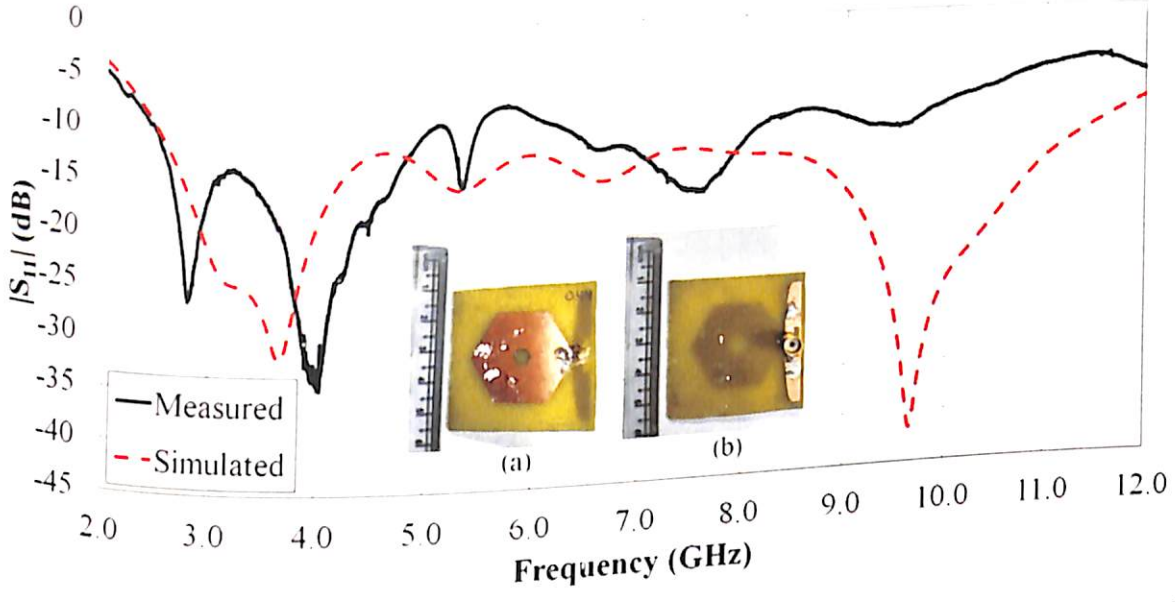

Figure 5.13. Scattering Parameter, $|S_{11}|$ (in dB) for probe fed hexagonal monopole UWB antenna. inset [Picture of the designed antenna (a) Front (b) Back]

The farfield radiation pattern of the fabricated UWB antenna is measured using standard measurement technique in an anechoic environment. The farfield radiation patterns are measured for two orthogonal planes i.e. E-plane and the H-plane for proposed antenna design for frequencies 2.3 GHz, 2.76 GHz, 4.11 GHz, 5.41 GHz, 8.4 GHz and 9.62 GHz as shown in Figure 5.14. The farfield gain (dB) is calculated using the Friss transmission equation. The frequencies 2.3 GHz and 2.76 GHz represents TM_{11} mode. The farfield radiation pattern shows that the antenna posses monopole like radiation characteristics which make the proposed antenna suitable for UWB application.

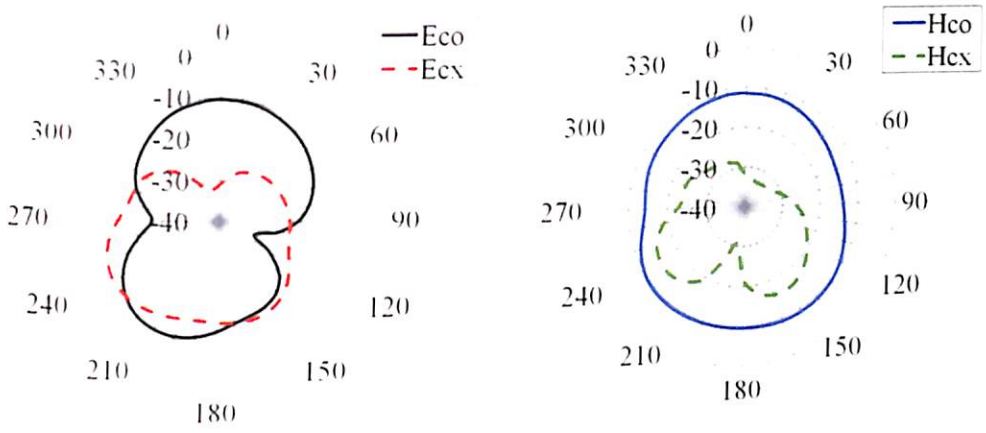

(a) 2.3 GHz

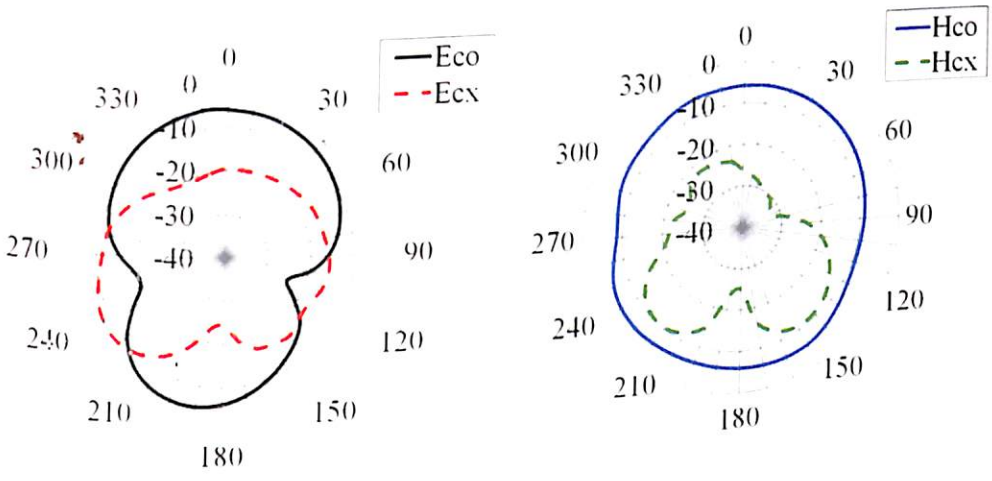

(b) 2.76 GHz

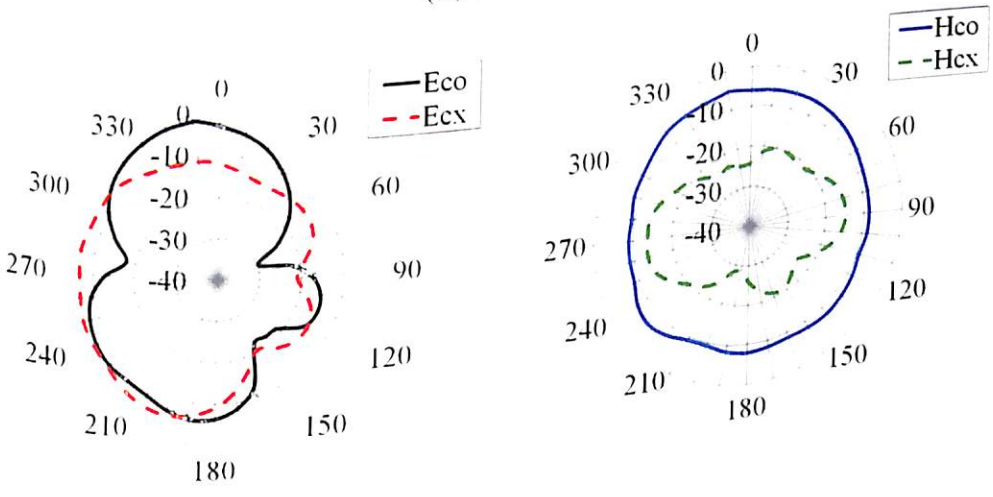

(c) 4.11 GHz

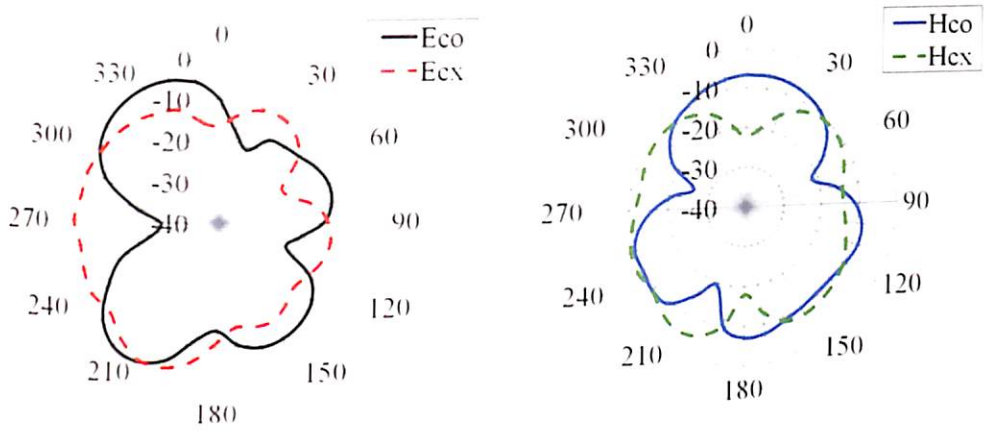

(d) 5.41 GHz

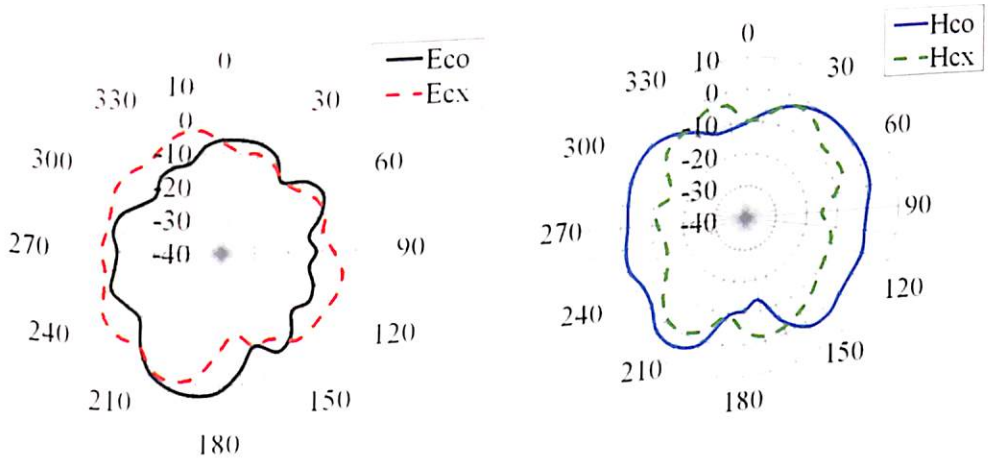

(e) 8.4 GHz

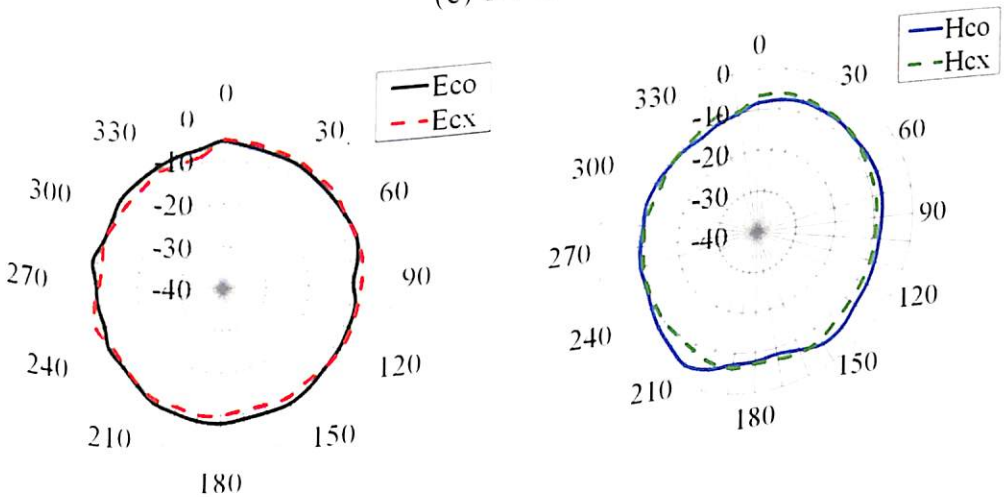

(f) 9.62 GHz

Figure 5.14. Measured farfield gains (dB) for proposed antenna.

5.4. Lowest Edge Resonance Frequency of Probe Fed Printed Monopole Antenna

Stripline fed quarter wave hexagonal monopole antenna was modeled in (Ray 2010) and the empirical formula to calculate lower edge frequency (f_l in GHz) of stripline fed hexagonal monopole antenna given in (Ray 2010). Equation (5.1) can be used to calculate the lower band edge frequency (f_l in GHz) of the designed antenna.

$$f_L = \frac{7.2}{k(L+h_{reff})} \tag{5.1}$$

where, $L = 2\times h_r$, $h_{reff} = ((h_r\times 3\sqrt{3})/(8\pi))$ are in cm and empirical value, k = 1.15, for a stripline fed at the vertex of the printed hexagonal monopole antenna.

Table 5.2. Comparison of f_l of various monopole antenna configuration.

Antenna Configuration	Measured / Simulated f_L (GHz)	Calculated f_L (GHz) using			Percentage Error in f_L using		
		(Ray 2009)	(Ray 2010)	(Zhantao 2008)	(Ray 2009)	(Ray 2010)	(Zhantao 2008)
Rectangle in (Ray 2009)	1.5	1.35	0.92	1.55	-10	-38.8	+3.3
Hexagon in (Ray 2010)	1.1	1.06	1.0743	0.8975	-3.8	-2.336	-18.41
Circular in (Zhantao 2008)	2.65	3.40	2.54	2.65	+28.3	-4.2	+1.766

Due to hexagonal area equated to equivalent circular area, the empirical value of 1.15 for FR-4 substrate is multiplied in the denominator to calculate the lowest edge frequency of the stripline fed hexagonal monopole antenna when fed at the vertex of hexagon. Instead of the length 0.25λ i.e. quarter wave, 0.24λ is used in the formula which results in 7.2 in the numerator. In case of printed monopole antenna the lower edge frequency is significant

parameter rather than the resonant frequency. The lower edge frequency of a printed monopole antenna is given by

$$f_L = \frac{c}{\lambda\sqrt{\varepsilon_{eff}}} \tag{5.2}$$

where, c is the speed of light. But, here quarter wave monopole antenna is used. The Length will be $L = \lambda/4$, thus $\lambda = 4L_{eff}$, therefore

$$f_L = \frac{c}{4L_{eff}\sqrt{\varepsilon_{eff}}} \tag{5.3}$$

$$f_L = \frac{7.5}{L_{eff}\sqrt{\varepsilon_{eff}}} \tag{5.4}$$

In case of stripline fed monopole antenna, the effective length will be $L_{eff} = L + L_s$ and hence the lower edge frequency is given by

$$f_L = \frac{7.5}{(L+L_S)\sqrt{\varepsilon_{eff}}} \tag{5.5}$$

where, $\varepsilon_{eff} = (\varepsilon_r - 1)/2$ and Ls is the length of the stripline.

The f_L is found to be 1.72 GHz, when $h_r = 1.65$ cm.

The dimensions of the hexagon mention earlier are chosen in order to accommodate entire S-Band. But, after fabrication, the f_L calculated using equation (5.1) provides an error of 25.21%, because probe feeding is used for the excitation of the hexagonal monopole antenna. Suitable expression for the calculation of f_L for probe fed hexagonal monopole antenna is not available in the literature.

Table 5.3. Comparison of f_l of various monopole antenna configurations using modified formula.

Antenna Configuration	Measured / Simulated f_L (GHz)	Calculated f_L (GHz) using expression		Percentage Error in f_L for expression	
		(5)	(6)	(5)	(6)
Rectangle in (Ray 2009)	1.5	1.46	1.55	-2.7	+3.3
Hexagon in (Ray 2010)	1.1	1.107	1.11	+0.6	+0.9
Circular in (Zhantao 2008)	2.65	3.51	2.65	+32.4	+1.766

For the formulation of probe fed hexagonal monopole antenna the empirical value is avoided by assuming it as a '1' which was earlier used in stripline fed hexagonal monopole antenna, due the fringing extension and the effective dielectric constant ($1<\varepsilon_{eff}<\varepsilon_r$). The additional effective h_{reff} and feed line length is also avoided, since vertical probe is used to feed the vertex of hexagon. Another reason for choosing k = 1 is that, due to negligible capacitance of the patch due to monopole configuration and purely inductive patch the effective dielectric constant leads to 1. The basic formula for frequency is

$$f_L = \frac{7.5}{L_{eff}\sqrt{\varepsilon_{eff}}} \tag{5.6}$$

Hexagonal patch configuration can be modeled as an equivalent circular patch antenna. There, the resonance frequency depends on the equivalent circular modes represented by the Bessel function. For a vertex fed hexagonal monopole antenna, the length of hexagon will be twice the circumradius of the hexagon i.e. $L = 2\times h_r$, substituting in expression (5.6) results in

$$f_L = \frac{c}{4(2h_r)\sqrt{\varepsilon_{eff}}} \tag{5.7}$$

Although expression for vertex fed hexagonal monopole have been explored earlier and empirically, derived for a stripline fed antenna, here we are presenting an empirical formula which is more suited to a probe fed hexagonal monopole antenna when fed at vertex of hexagon.

$$f_L = \frac{7.5}{2h_r\sqrt{\varepsilon_{eff}}}$$

or

$$f_L = \frac{3.75}{h_r\sqrt{\varepsilon_{eff}}} \tag{5.8}$$

where, h_r is in cm. The empirical expression given in expression can be justified by the fact that the monopole can be modeled as a pure inductance with negligible capacitive effect.

$$f_L = \frac{3.75*(1.52+\left(\frac{ln\left(\frac{b}{a}\right)}{2\pi}\right))}{(h_r+L_p)\sqrt{\varepsilon_{eff}}} \tag{5.9}$$

Moreover, the higher edge frequency of the impedance bandwidth of the probe fed hexagonal antenna can also be estimated using the following formula empirical formula.

(5.10)

$$f_H = \frac{c}{h_r\sqrt{\varepsilon_{eff}}}$$

where, c is the light speed in free space and $\varepsilon_{eff} = (\varepsilon_r + 1)/2$.

The expression in (5.9) is used to calculate the f_L for three planar monopole antennas i.e. square, circle, and hexagon. All the three antenna configurations are assumed to have the same circumradius of 16.5 mm. The calculated values of f_L are indicated in Table 5.4. The value of f_L are further verified through CST simulation results.

Table 5.4. Comparison of f_l of proposed probe fed monopole antenna configurations using proposed formula.

Antenna Configuration	Simulated f_L (GHz)	Calculated f_L (GHz) using Expression (5.10)	Percentage Error in f_L
Rectangle	2.3	2.27	-1.3
Circle	2.4	2.27	-5.41
Hexagon	2.3	2.27	-1.3

Three different probe fed monopole antenna configurations i.e. rectangle, circle, and hexagon with feed position at vertex of polygon are designed in CST microwave studio as shown in inset of Figure 5.15 and simulated for S_{11} characteristics as reflected in Figure 5.15. The probe at vertex of polygon helps in designing the monopole antenna by avoiding overlapping with the ground. The patch has been modeled as a regular design with circumradius h_r. The three configurations designed consists of a FR-4 substrate of 46 × 46 mm^2 and a ground plane with dimension 3 × 40 mm^2 and a patch with circumradius 16.5 mm. The ground dimensions of the antenna configurations are chosen such that the designed probe fed hexagonal monopole antenna have minimum size. All the three antennas have the almost same lowest edge frequency as may be observed from Figure 5.15 at -10 dB and indicated in Table 5.4.

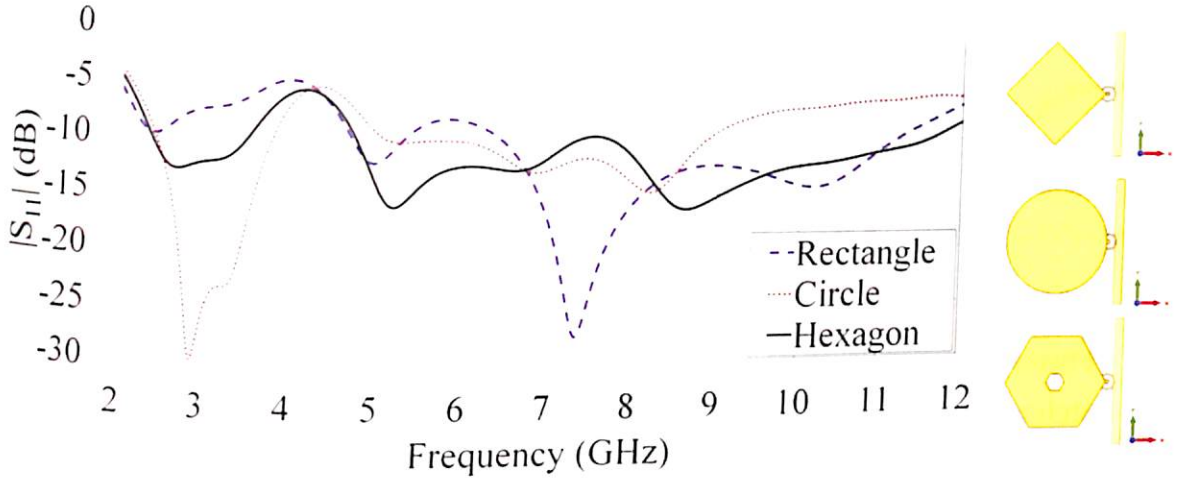

Figure 5.15. Scattering Parameter, $|S_{11}|$ (in dB) of different monopole antenna configurations [Inset: Pictures of antennas].

Expression (5.8) is found to be more suitable for a probe fed hexagonal monopole antenna especially when fed at vertex of hexagon which yields, f_L = 2.27 GHz when substituted in equation (5.8), which provide an error of 1.3 % as indicated in Table 5.4. As observed from Figure 5.15 the that probe fed hexagonal monopole antenna possess the wideband characteristics and further chosen for fabrication to design probe fed UWB monopole antenna. The hexagon monopole antenna shows weak rejection at 4.3 GHz as depicted from Figure 5.15.

The probe fed hexagonal monopole antenna is fabricated as shown in inset of Figure 5.16, because it provide UWB band as observed in earlier section. The lower edge frequency of the probe fed hexagonal monopole antenna is validated using measurement results obtained from VNA which is 2.3 GHz. The simulated and measurement S_{11} (dB) results are also compared and presented in Figure 5.16.

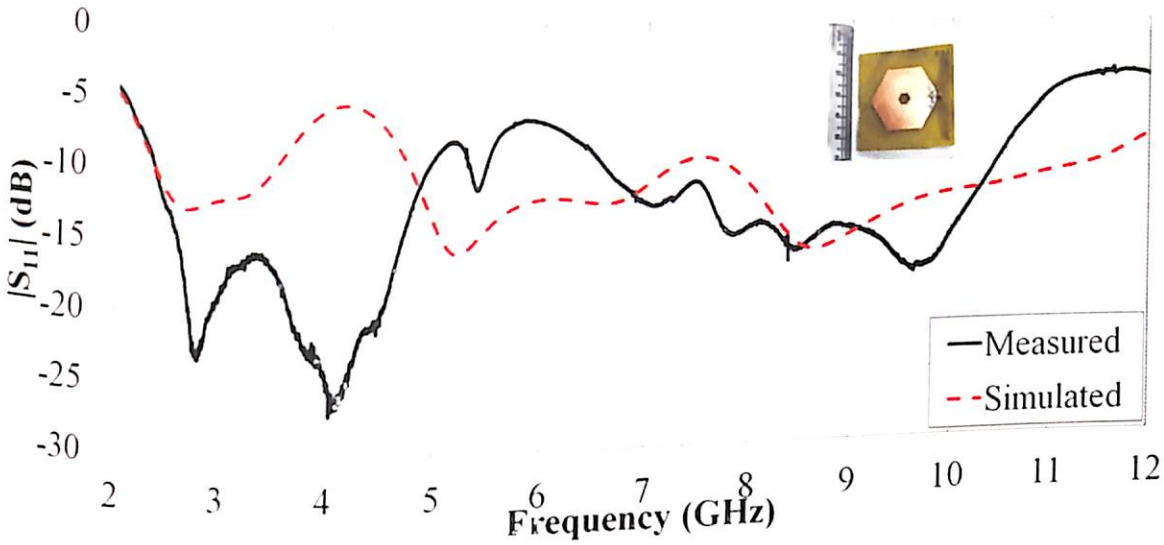

Figure 5.16. Scattering Parameter, $|S_{11}|$ (in dB) for probe fed hexagonal monopole antenna [Inset: Picture of the fabricated probe fed hexagonal monopole antenna].

The lower edge frequency is exactly same for the simulated and measured results, i.e., 2.3 GHz as depicted from Figure 5.16 and hence, proves the validity of the proposed expression for the calculation of lower edge frequency of probe fed monopole antenna design, especially, when fed at the vertex of hexagon. The weak rejection is shifted to 5 GHz due to fabrication tolerances. The designed probe fed hexagonal monopole antenna cover the entire UWB band i.e. 2.3 GHz to 10.6 GHz.

5.5. Probe-fed Hexagonal UWB Antenna with AMC Reflector

The hexagonal UWB antenna with probe feed is designed as shown in Figure 5.17 with a height, h_1 = 1.5 mm and size of 46 × 46 mm^2 to be developed on a FR-4 substrate. The hexagon circumradius is 16.5 mm with a hexagonal slot radius of 3 mm for slight improvement of antenna's gain as suggested in (Joshi 2015c). In order to achieve UWB monopole antenna, the half elliptical ground of radius, e_r = 2.5 mm with a rectangular slot of dimension, 2 × 10 mm^2 are optimized. The loop AMC unit cell has a outer dimension of 4.55 × 4.55 mm^2 while the inner slot has a dimension of 3.8 × 2.05 mm^2 and inter-element spacing between the unit cell is 0.075 mm as shown in inset of Figure 5.17(a).

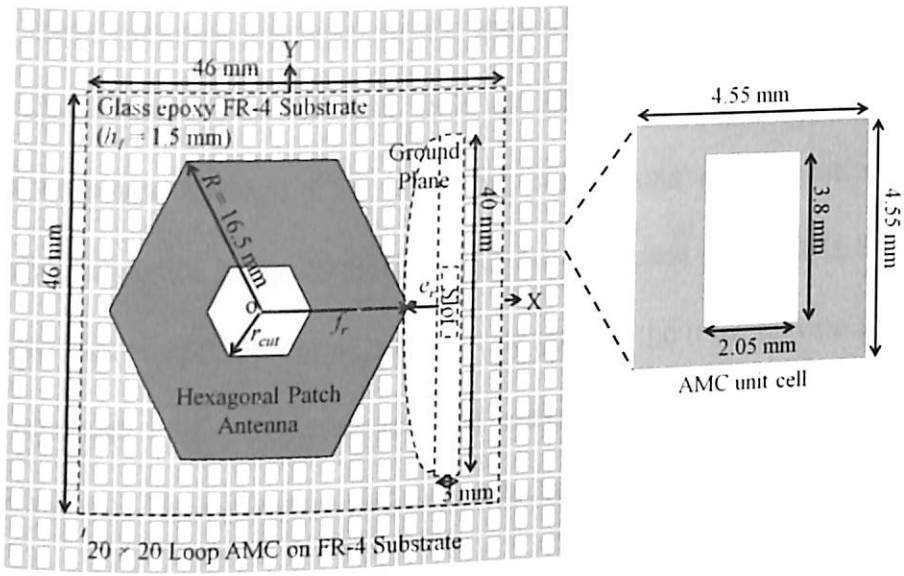

(a)

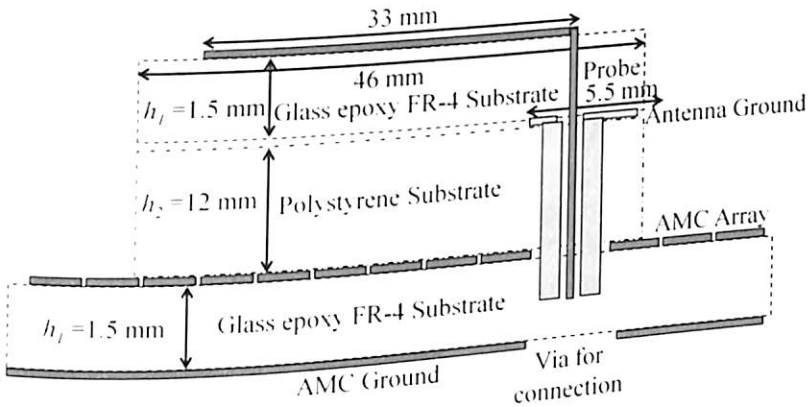

(b)

Figure 5.17. Proposed multilayered antenna structure with dimensions (a) Sectional view, zoomed out view of AMC unit cell in the inset, (b) Side view.

The 20 × 20 AMC array is also fabricated on similar FR-4 substrate with height, h_1 = 1.5 mm. The polystyrene substrate with thickness, h_2 = 12 mm is sandwiched between the antenna structure and the AMC structure as shown in Figure 5.17(b). A SMA connector without flanges is used to feed the vertex of the hexagon i.e., f_r = 17 mm. The circular via of diameter 12 mm is created in the AMC structure, in order to connect SMA cable.

To analyse the AMC unit cell on S_{11} (dB) reflection characteristics and S_{21} (dB) transmission characteristics, the value of parameters l_u, s_2, and g are kept constant and simulated using CM. The S_{11} (dB) reflection characteristics and transmission characteristics

S_{21} of AMC array obtained through circuit model is compared with those obtained and observed in CST simulations of unit cell as shown in Figure 5.18. The reflection characteristics obtained through CST and CM simulations are almost same, while the transmission characteristics suggests that cut off starts between 5 to 6 GHz for both CST and CM simulations. Due to application of polystyrene spacer, the transmission cut off shifts to a higher value between 6 to 7 GHz as per CM which is supported by observations during pattern measurements. The reflection and transmission characteristics of AMC unit cell with polystyrene layer (indicated by -P suffix) is shown in Figure 5.18 for both CM and CST simulations. The reflection and transmission characteristics obtained through CST simulations demonstrate the validity of the circuit model of AMC array, which estimates the frequency response of its structure. The square loop unit cell element with an edge length, l_u = 4.55 mm, different inner edge widths, s_1 = 0.375 mm; s_2 = 1.25 mm and an inter-element spacing, g = 0.075 mm has been selected to form a 20×20 array as shown in Figure 5.17(a).

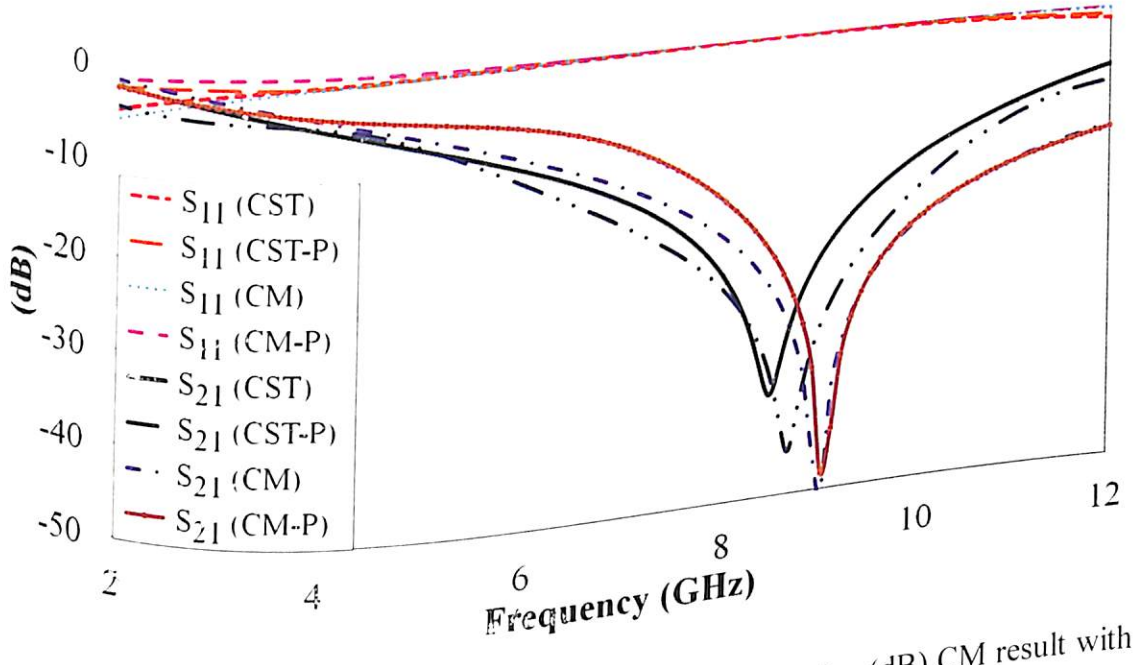

Figure 5.18. Comparison of loop AMC unit cell S_{11} (dB) and S_{21} (dB) CM result with CST results.

The hexagonal monopole antenna and the AMC array is separated by a polystyrene spacer and the thickness of the polystyrene spacer, h_2 = 12 mm, is calculated from the AMC array simulated S_{11} characteristics such that there will be additive phase between the radiated and the reflected wave from the AMC reflector ($\phi_{AMC} - 4\pi h_2/\lambda - \pi = 2N\pi$, where N = 1, 2, 3,...).

The standard PCB development technique is used to develop AMC and the antenna is displayed in Figure 5.19. The overall dimension of the developed antenna with AMC is 100 × 100 mm^2.

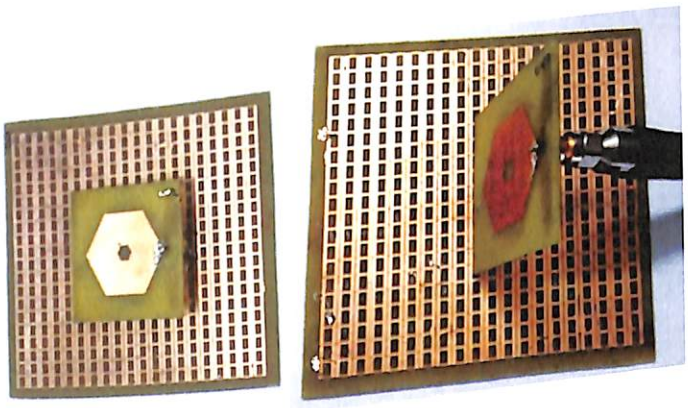

Figure 5.19. Images of the developed antenna with AMC.

The scattering parameter, $|S_{11}|$ (in dB) of the antenna with AMC and without AMC are simulated and compared in order to observe the consequence of loop AMC reflector and antenna together on $|S_{11}|$ (in dB) as reflected in Figure 5.20. The simulated bandwidth $|S_{11}| < -10$ is observed from 2.4 GHz to 11.8 GHz for the hexagonal monopole antenna with AMC and without AMC. There is no significant difference between the simulated impedance bandwidth of the antenna with AMC and without AMC as observed from Figure 5.20. Furthermore, measured $|S_{11}|$ (in dB) are compared for the designed antenna in presence and absence of AMC and shown in Figure 5.20. The $|S_{11}| < -10$ dB of antenna without AMC ranges from 2.4 to 11.8 GHz i.e. covering complete UWB band, while the measured $|S_{11}| < -10$ dB with AMC ranges from 2.7 GHz to 11.8 GHz as reflected in Figure 5.20, with a slight

deterioration at around 5.5 GHz is observed due to application of AMC with polystyrene which may be seen as a weak rejection of the band of frequencies near 5.5 GHz.

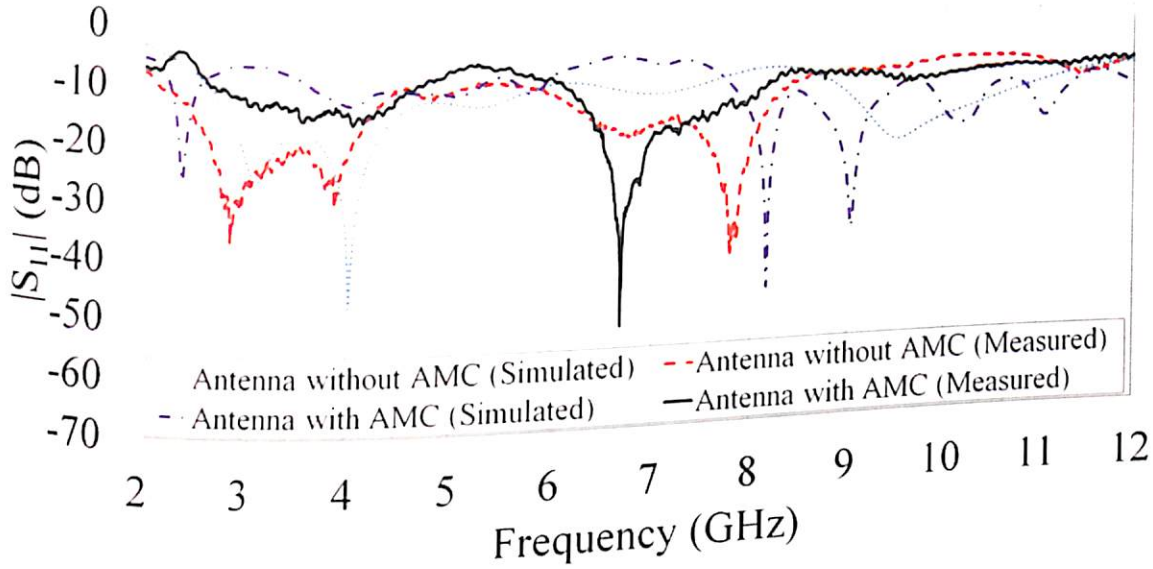

Figure 5.20. Scattering Parameter, $|S_{11}|$ (in dB) for probe-fed hexagonal monopole UWB antenna.

A qualitative difference between the antenna with and without AMC is observed due to unavoidable assembling misalignments and tolerances during prototype fabrication. However, the impedance matching slightly deteriorates in the presence of the AMC at lower frequencies UWB frequencies. Moreover, the deterioration is also evident in case of the measured results. It is significant to note that the operating region of the AMC is 6.2 to 12 GHz, where reflection is maximum, impedance mismatch due to induced currents from reflected radiation with varying phase can be expected.

In order to understand the gain enhancement phenomenon due to AMC reflector, the boresight and peak gain of the hexagonal monopole antenna in absence and presence of AMC reflector are compared and displayed in Figure 5.21 and Figure 5.22. respectively. It is quite visible in Figure 5.21 AMC reflector improves average boresight gain by around 5.46 dB in simulation. The positive boresight gain of the antenna ranges from 2.2 GHz to 4.3 GHz

without AMC reflector while with AMC, a wider band from 2 GHz to 5.8 GHz is observed. A significant enhancement of boresight gain for a wider band is observed which suggests significance of an AMC reflector. In order to understand the effect of AMC on boresight gain enhancement, the boresight gain of the antenna in presence and absence of AMC is measured and presented as shown in Figure 5.21.

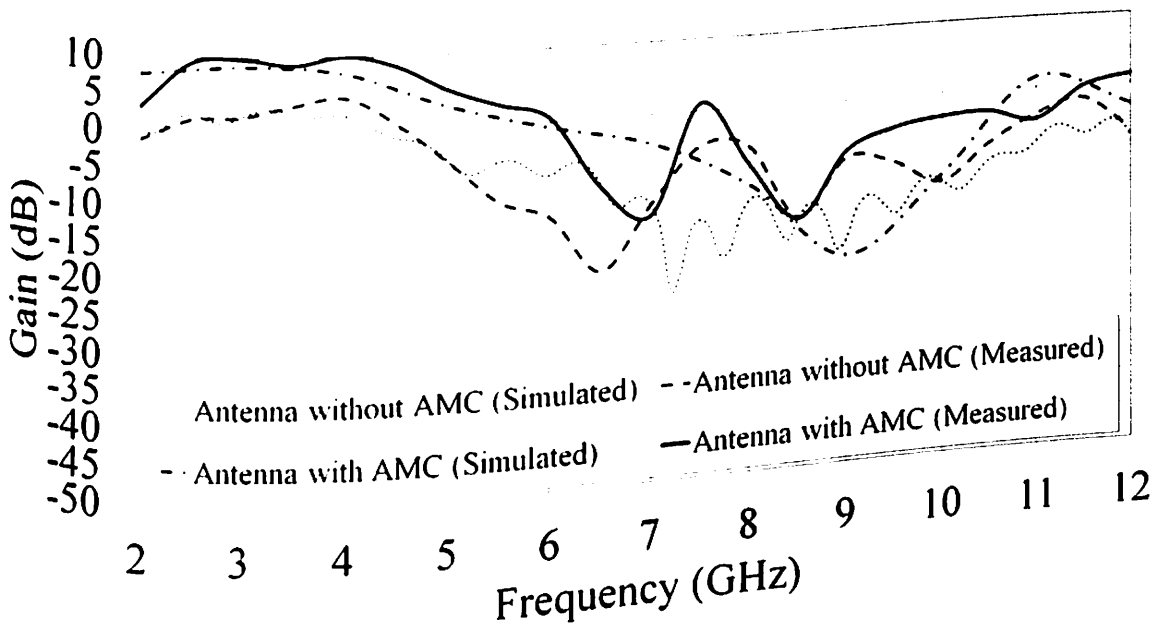

Figure 5.21. Measured Boresight gain, Gain (in dB) for probe-fed hexagonal monopole UWB antenna.

The antenna's boresight gain appears positive for a wide band that ranges from 2 GHz to 6 GHz during measurements as compared to 2.2 GHz to 4.5 GHz when no AMC reflector was applied. It is observed during measurements that average boresight gain is enhanced by a magnitude of 5.5 dB due to application of AMC in hexagonal monopole antenna.

Comparison of simulated peak gain (dB) results of the antenna in presence and absence of AMC shows that the average peak gain is enhanced by a magnitude of 3.52 dB as may be observed from Figure 5.22. The peak gain increases with the frequency in antenna with and

without AMC due to its higher physical aperture area. Proposed antenna's peak gain with and without AMC are compared and the gain enhancement is quite visible in Figure 5.22.

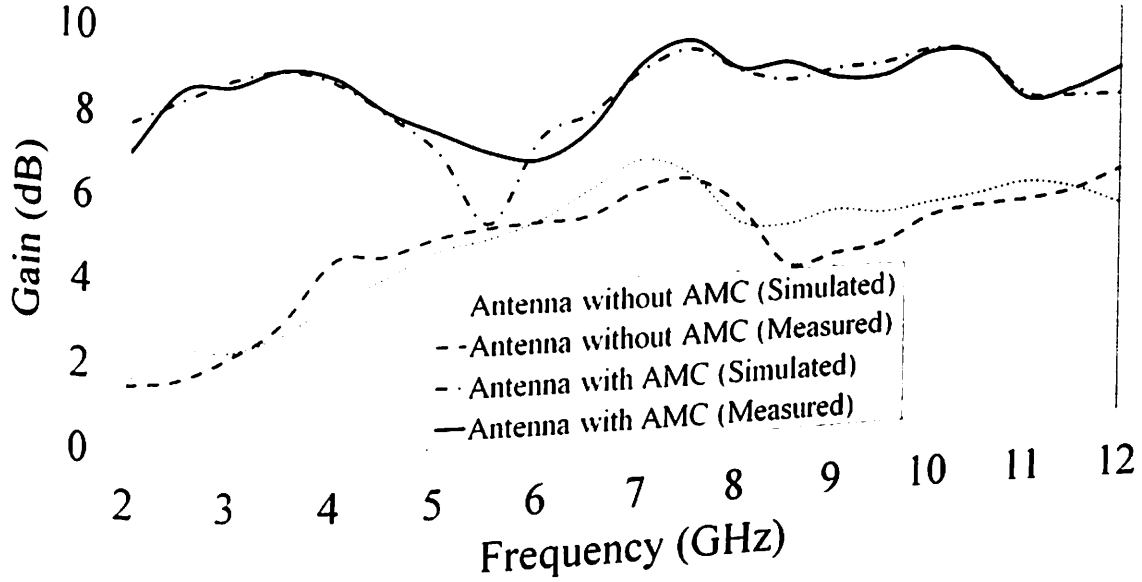

Figure 5.22. Measured Peak Gain (in dB) for probe-fed hexagonal monopole UWB antenna.

It is clear from the measured peak and boresight gain results that an AMC reflector plays a notable role in the gain improvement of a hexagonal UWB monopole antenna. The average peak gain is enhanced by 3.74 dB when observed during measurement.

Quantative differences between simulated and measured results are observed due to practical limitations and fabrication tolerances. Critical parameters responsible for differences in S_{11} and gain curves are non uniformity in height of polystyrene, quality of polystyrene, location of feed, inter-element spacing among AMC unit cells, patch and ground plane overlap. To explicitly demonstrate the performance of the designed antenna with AMC, a comparison is done with similar antenna configurations where dimensions of antenna and reflector, spacing between antenna and reflector, S_{11} bandwidth, and the average gain enhanced are compared within the operating band of each antenna in Table 5.5.

Table 5.5. Gain comparison of antennas backed by reflectors in reported literature

Reference Work	Antenna Dimensions (mm^2)	Reflector Dimensions (mm^2)	Antenna - Reflector Spacing (mm)	Antenna Bandwidth (GHz)	Average Peak Gain Enhanced (dB)
(Tahir 2017)	26 × 34	~90 × 90	30	11.4	3.8
(Tahir 2016)	25 × 40	~60 × 50	10	18	4.5
(Krishna 2015)	30 × 60	~145 × 145	15	8.8	2.21
(Krishna 2014)	40 × 40	~100 × 100	21	7.9	4.24
(Ranga 2011)	63 × 63	~120 × 120	(i) 9.5 (ii) 8.5	9.5	2.19
(Ranga 2013)	63 × 63	~120 × 120	(i) 19 (ii) 1.58 (iii) 1.58	15	2.84
(Sen 2017)	40 × 40	~100 × 50	22	7.5	5.32
This work	46 × 46	100 × 100	15	9.3	3.74

It is significant to note that most of the work reported earlier has expressed only antennas' peak gain to describe technique of the gain enhancement. A strong reflection is introduced within the operating band in most designs, and the gain performance is enhanced. The average peak gain enhanced is either higher or comparable to that expressed in earlier reports. It is significant to note that the average boresight gain is also enhanced by a magnitude of 5.5 dB due to presence of AMC reflector.

To analyze the effect of AMC on the radiation patterns of the fabricated antenna, radiation pattern measurements of antenna assembled in presence and absence of AMC in an anechoic environment using the same measurement setup presented in chapter 3 and chapter 4, as shown in Figure 5.23 are performed at different frequencies when $|S_{11}| \leq -15$ dB.

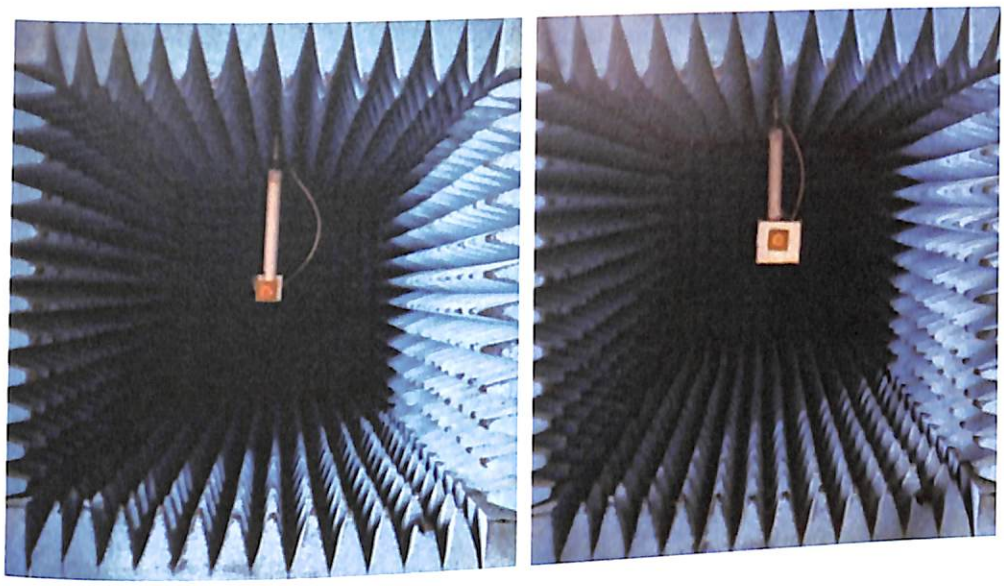

(a) (b)

Figure 5.23. Antenna with AMC and without AMC in anechoic environment.

The farfield gain of the fabricated antenna with and without AMC for two orthogonal planes i.e. XOZ-plane and the YOZ-plane is measured at different frequencies in the operating band using standard measurement technique. The measured radiation patterns are displayed in Figure 5.24. To calculate the farfield gain (dB), the well known Friss transmission equation is used as given in (Balanis 2016). The radiation pattern for XOZ-plane and the YOZ-plane for antenna without AMC is bidirectional with back lobes at lower frequencies while at higher frequencies, the power is radiated in all directions but with poor gain. Due to application of AMC it is observed that the black lobes at $\theta = 180^{\circ}$ for both XOZ-plane and the YOZ-plane of the hexagonal monopole antenna are significantly reduced and the radiation pattern becomes directional. It is interesting to note by observing Figure 5.24 that by application of AMC both co- and the cross-polar components are enhanced in both E- and H-plane.

The radiation pattern of UWB hexagonal monopole antenna presented in Figure 5.14 have bidirectional radiation pattern but due to application of AMC the back lobe reduces significantly as may be observed from Figure 5.24.

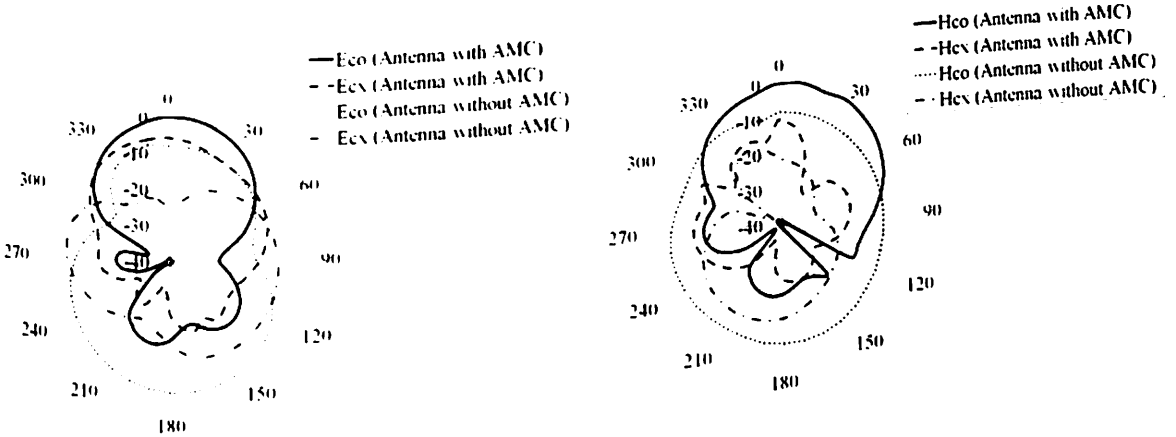

(a)

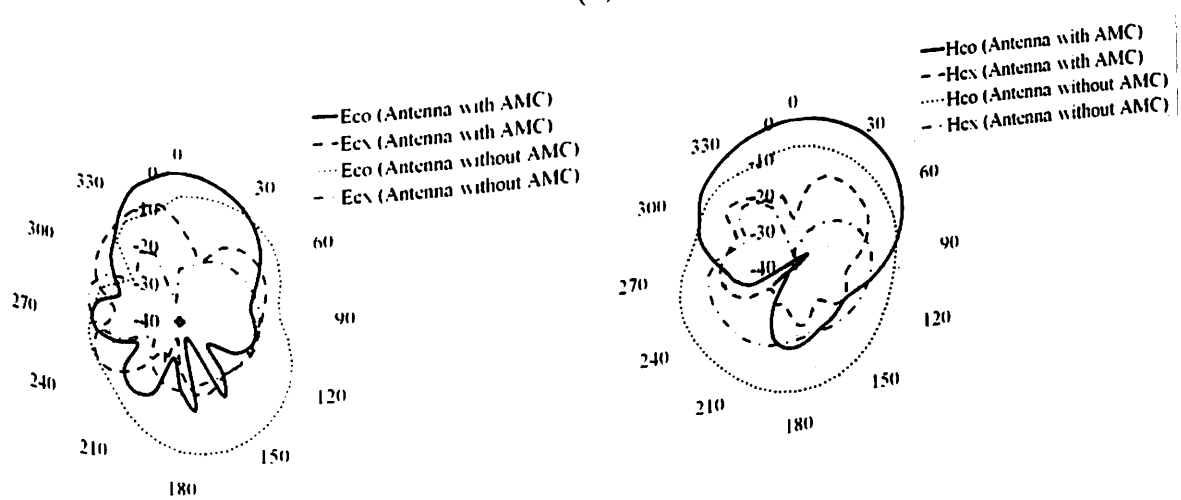

(b)

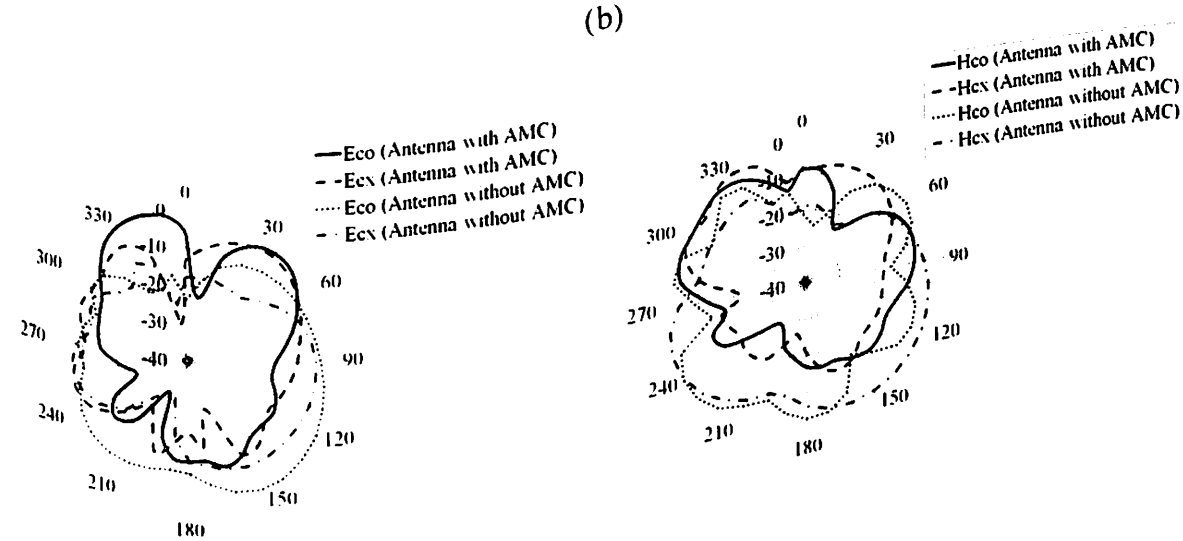

(c)

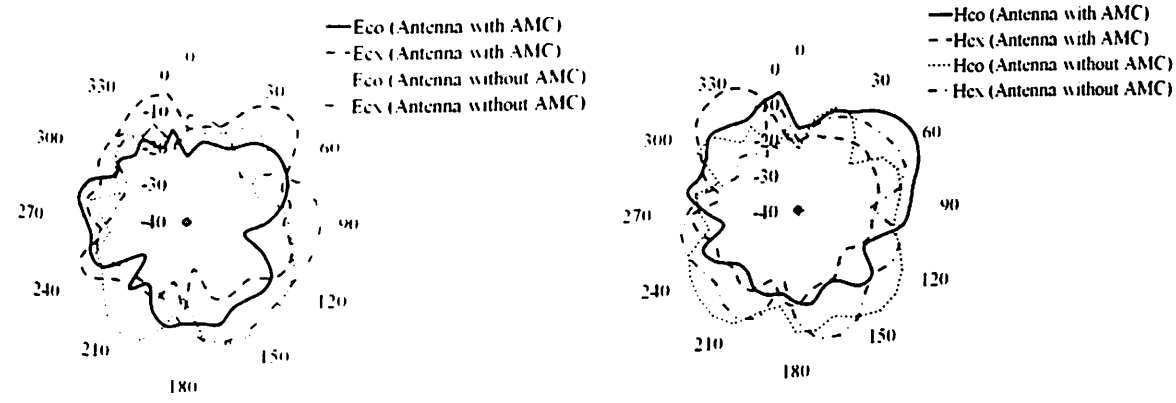

(d)

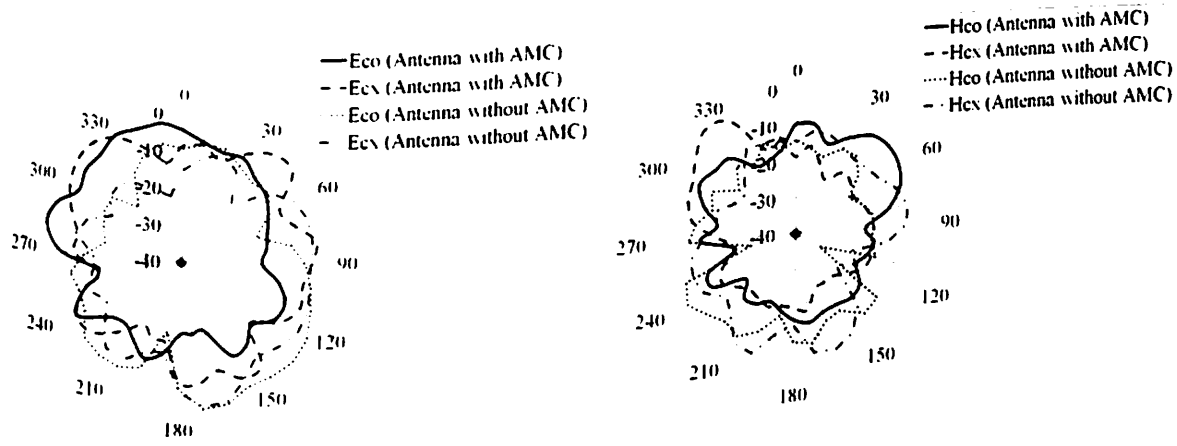

(e)

Figure 5.24. Measured radiation patterns of antenna in XOZ-plane and YOZ-plane with/without AMC at different frequencies (in GHz) (a) 3.3 (b) 4.1 (c) 6.2 (d) 8.4 (e) 9.5.

5.6. Conclusion

This chapter demonstrates a ground modification technique to achieve almost flat and uniform gain within the wide operating band of a hexagonal S-band monopole antenna. A simple empirical formula has been presented to accurately predict the lower edge frequency of probe fed regular hexagonal monopole antenna, when fed at the vertex of hexagonal which is quite close to the simulated and measured $|S_{11}|$ results of the designed antenna. The feed point variation near the vertex of hexagon has been studied and presented to achieve maximum bandwidth. The ground modification excites lower frequencies, which merge to

form a wideband with an impedance bandwidth of 2.6 GHz. The designed low profile S-band antenna can provide positive boresight gain from 2.1 GHz to 4.6 GHz, which covers the impedance bandwidth as mentioned earlier and positive peak gain for the S-band.

In this chapter, the effect of flanges of a SMA connector on the impedance bandwidth of a vertex-fed slotted hexagonal antenna with a truncated half elliptical ground plane is demonstrated. The proposed antenna when fed through a connector with a flange exhibits C-band characteristics while in order to achieve UWB characteristic in a direct-fed antenna, a flangeless connector makes a suitable choice. A technique to achieve ultra wideband in a vertex fed hexagonal patch antenna directly fed with probe is demonstrated. The feed point optimization technique is demonstrated to excite all possible modes of the hexagon. The technique to reduced ground plane that transforms antenna to a monopole structure and a modified probe, both are used to achieve ultra wideband. The slot in the ground plane supported broadening of the bandwidth of the antenna. A ground plane reduction technique is used with a rectangular slot to excite multiple modes within the UWB band. The proposed antenna, exhibits a wideband from 2.4 GHz to 10 GHz.

A simple empirical formula has been presented to accurately calculate the lower edge frequency of probe fed regular hexagonal monopole antenna, when fed at the vertex of hexagonal which is quite close to the simulated and measured $|S_{11}|$ results of the designed antenna. The expression to calculate the effective dielectric constant and the lowest edge resonant frequency of probe fed VHMA is validated using measurement.

A technique to transform a monopole like radiation pattern to a directional pattern using an AMC reflector with a square shaped loop unit cell, consequently enhancing the gain of the hexagonal UWB antenna is presented. An AMC reflector with 20 × 20 array of unit cells is assembled at back of hexagonal radiator in order to enhance the peak gain as well as gain of the UWB antenna. The proposed antenna boresight and peak gain are significantly enhanced

by around 5.5 dB and 3.74 dB respectively after application of AMC reflector. The assembled antenna with AMC is suitable to be exploited for UWB applications.